CHAPTER

Static Equilibrium and Trim

3

3.1 Trim equilibrium

When considering the short term dynamic stability and control characteristics of an aircraft it is usual to refer the motion to a steady trimmed flight condition. An essential prerequisite, therefore, is to define trim and to set out the conditions for the aircraft to remain in stable equilibrium.

3.1.1 Preliminary considerations

In normal flight it is usual for the pilot to adjust the controls of an aircraft such that on release of the controls it continues to fly steadily at the chosen flight condition. By this means the pilot is relieved of the tedium of constantly adjusting control inputs to maintain equilibrium and of holding the associated control forces, which may be tiring. The aircraft is then said to be *trimmed*, and the trim state defines the initial equilibrium condition about which the dynamics of interest may be studied. All aircraft are equipped with a means for presetting, or adjusting, the *datum*, *equilibrium*, or *trim* setting of the primary control surfaces. The ailerons, elevator, and rudder are all fitted with *trim tabs* for this purpose, which in all but the simplest aircraft may be adjusted from the cockpit in flight. However, all aircraft are fitted with a continuously adjustable elevator trim tab for the maintenance of longitudinal trim, which is continuously variable with flight condition.

It is an essential requirement that an aircraft must be stable if it is to remain in equilibrium following trimming. In particular, the static stability characteristics about all three axes largely determine the *trimmability* of an aircraft, and the *degree* of static stability determines, in part, the pilot control actions required to establish trimmed equilibrium. Thus *stability* characteristics and *control* characteristics are completely interdependent and both are determined by the aerodynamic design of the aircraft and by the action of a control and stability augmentation system when fitted. Dynamic stability is also important, of course, and largely determines the characteristics of the transient motion following a disturbance about a trimmed flight condition.

The object of trimming is to bring the forces and moments acting on the aircraft into a state of balance, or equilibrium. That is the condition when the net axial, normal, and side forces, and the net roll, pitch, and yaw moments are all zero. The force balance is often expressed approximately as the requirement that the lift equal the weight and the thrust equal the drag since, by definition, the net side force must be zero in trimmed symmetric flight. Provided the aircraft is stable, it will then remain in equilibrium until it is disturbed by pilot control inputs or by external influences such as turbulence. The transient motion following such a disturbance is characterised by the dynamic stability characteristics, and the stable aircraft will eventually settle into its equilibrium state once more.

The maintenance of trimmed equilibrium requires the correct simultaneous adjustment of the main flight variables in all six degrees of freedom and is dependent on airspeed, or Mach number, flight path angle, airframe configuration, weight, and *cg* position. As these parameters change during the course of a typical flight, trim adjustments are made as necessary. Fortunately, the task of trimming an aircraft is not as challenging as it might at first seem. The symmetry of a typical airframe confers symmetric aerodynamic properties on the airframe, which usually reduces the task to that of longitudinal trim only. Lateral-directional trim adjustments are only likely to be required when the aerodynamic symmetry is lost as a result, for example, of loss of an engine in a multi-engined aircraft.

Lateral-directional stability is designed into most aircraft and ensures that in roll the aircraft remains *wings-level* and that in yaw it tends to *weathercock* into wind when the ailerons and rudder are at their zero or datum positions. Thus, under normal circumstances, the aircraft will naturally seek lateral-directional equilibrium without interference by the pilot. This applies even when significant changes are made to airspeed, configuration, weight, and *cg* position, for example, since the symmetry of the airframe is retained throughout. However, such variations in flight condition can lead to dramatic changes in longitudinal trim.

Longitudinal trim involves the simultaneous adjustment of elevator angle and thrust to give the required airspeed and flight path angle for a given airframe configuration. Equilibrium is achievable only if the aircraft is longitudinally stable, and the magnitude of the control action to trim depends on the *degree* of longitudinal static stability. Since the longitudinal flight condition is continuously variable, it is very important that trimmed equilibrium is possible at all conditions. For this reason, considerable emphasis is given to the problems of ensuring adequate longitudinal static stability and adequate longitudinal aerodynamic trim control. Because of its importance, the generic description *static stability and trim* is often interpreted to mean *longitudinal static stability and trim*.

The commonly used theory of longitudinal static stability was developed by Gates and Lyon (1944) and derives from a full static and dynamic stability analysis of the equations of motion of an aircraft. An excellent and accessible summary of the findings of Gates and Lyon is given in Duncan (1959) and in Babister (1961). In the interest of understanding and physical interpretation, the theory is often reduced to a linearised form that retains only the principal aerodynamic and configuration parameters. It is in this simplest form that the theory is reviewed here since it is only required as the basis on which to build the small-perturbation dynamics model. It is important to appreciate that, although the longitudinal static stability model is described only in terms of the aerodynamic properties of the airframe, the control and trim properties as seen by the pilot must conform to the same physical interpretation even when they are augmented by a flight control system. It is also important to recognise that static and dynamic stability are, in reality, inseparable. However, the separate treatment of static stability is a useful means for introducing the concept of stability insofar as it determines the control and trim characteristics of the aircraft.

3.1.2 Conditions for stability

The static stability of an aircraft is commonly interpreted to describe its tendency to converge on the initial equilibrium condition following a small disturbance from trim. Dynamic stability, on the other hand, describes the transient motion involved in the process of recovering equilibrium following the disturbance. Fig. 3.1 includes two illustrations showing the effects of static stability and static instability in an otherwise dynamically stable aircraft. Following an initial disturbance

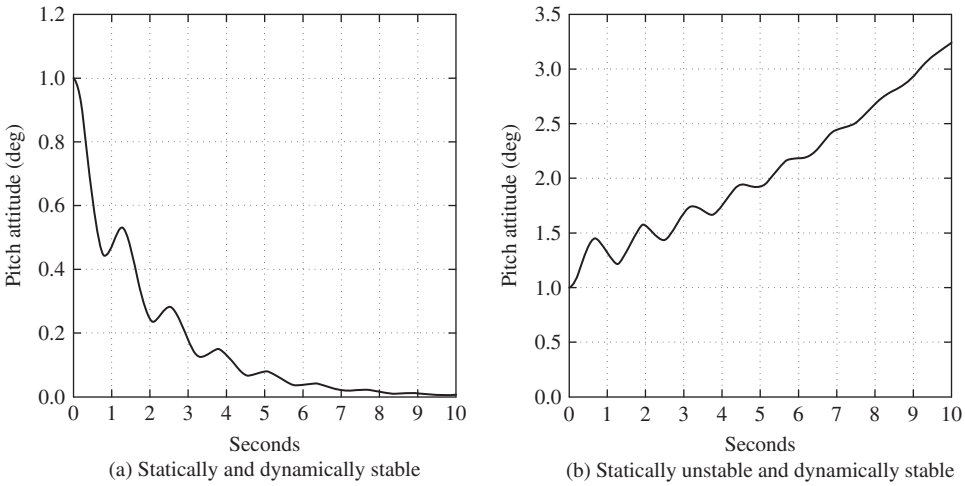

FIGURE 3.1 Stability.

displacement, in pitch for example, at time $t = 0$, the subsequent response time history is shown and is clearly dependent on the stability of the aircraft. It should be noted that damping of the dynamic oscillatory component of the responses shown was deliberately chosen to be low in order to best illustrate the static and dynamic stability characteristics.

In establishing trim equilibrium, the pilot adjusts the elevator angle and thrust to obtain a lift force sufficient to support the weight and thrust sufficient to balance the drag at the desired speed and flight path angle. Since the airframe is symmetric, the equilibrium side force is, of course, zero. Provided that the speed is above the minimum drag speed, the force balance will remain stable with speed. Therefore, the static stability of the aircraft reduces to a consideration of the effects of angular disturbances about the three axes. Following such a disturbance the aerodynamic forces and moments will no longer be in equilibrium, and in a statically stable aircraft the resultant moments will cause the aircraft to converge on its initial condition. The condition for an aircraft to be statically stable is therefore easily deduced.

Consider a positive incidence disturbance from equilibrium. This is in the nose-up sense and results in an increase in incidence α and hence in lift coefficient C_L. In a stable aircraft the resulting pitching moment must be restoring—that is, in the negative or nose-down sense. And, of course, the converse must be true following a nose-down disturbance. Thus the condition for longitudinal static stability may be determined by plotting the total aircraft pitching moment M or, equivalently, pitching moment coefficient C_m for variation in incidence α about the trim value α_e, as shown in Fig. 3.2. The nose-up disturbance increases α and takes the aircraft to the out-of-trim point p where the pitching moment coefficient becomes negative and is therefore restoring. This property describes the *pitch stiffness* of an aircraft. Clearly, a nose-down disturbance leads to a similar conclusion. As indicated, the aircraft is stable when the slope of this plot is negative. Thus the condition for stable longitudinal trim at incidence α_e may be expressed as

$$C_m = 0 \tag{3.1}$$

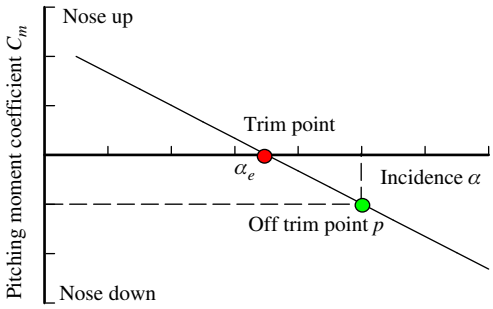

FIGURE 3.2 Pitching moment variation with incidence for a stable aircraft.

and

$$\frac{dC_m}{d\alpha} < 0 \tag{3.2}$$

The previous observation is strictly valid only when it is assumed that the aerodynamic force and moment coefficients are functions of incidence only. This is usually an acceptable approximation for subsonic aircraft and, indeed, the plot of total aircraft pitching moment coefficient against incidence may well be very nearly linear as shown in Fig. 3.2. However, this argument becomes increasingly inappropriate with increasing Mach number. As compressibility effects become significant, the aerodynamic force and moment coefficients become functions of both incidence and Mach number. When this occurs equation (3.2) may not always guarantee that stable trim can be achieved.

The rather more complex analysis by Gates and Lyon (1944) takes speed effects into account and defines a general requirement for longitudinal static stability as

$$\frac{dC_m}{dC_L} < 0 \tag{3.3}$$

For subsonic aircraft equations (3.2) and (3.3) are completely interchangeable since α and C_L are linearly, or very nearly linearly, related by the lift curve slope a.

Inspection of Fig. 3.2 indicates that it is not possible to achieve trim unless the zero-incidence ($\alpha = 0$) pitching moment coefficient for the aircraft is positive, which determines the additional constraint for a stable trimmable aircraft:

$$C_{m(\alpha=0)} > 0 \tag{3.4}$$

More generally, it is a requirement that the zero-lift ($C_L = 0$) pitching moment coefficient be positive as well for a trimmable aircraft:

$$C_{m(C_L=0)} > 0 \tag{3.5}$$

Now it is important to recognise that the pitching moment referred to in equations (3.4) and (3.5) is the *whole-aircraft* pitching moment, not to be confused with the *wing-body* zero-lift

($C_L = 0$) pitching moment coefficient, C_{m_0}, referred to in later sections of this chapter. The wing-body zero-lift pitching moment is assumed to be dominated by the aerodynamic properties of the wing, and for a typical wing having an aerofoil section with positive camber, C_{m_0} is negative. Thus, in order that the whole aircraft zero-lift pitching moment coefficient is positive, a tailplane is added and set at a local angle of attack sufficient to ensure stable trim over the operational flight envelope. An actual application is discussed in Example 3.1. Typically, a tailplane has a symmetric uncambered aerofoil section which contributes zero pitching moment at zero tail lift. Consequently, the tailplane contribution to total aircraft pitching moment is determined by its local angle of attack and by deflection of the elevator control surface only, and its magnitude is determined by the aerodynamic design choices relating to tail moment arm about the *cg* and by tailplane area. This concept defines the basis for the detailed analysis of pitching moment set out in Section 3.2.

The special case of tailless aircraft poses challenges if longitudinal static stability is to be achieved. Since a lifting wing requires an aerofoil section with positive camber, the problem of negative pitching moment remains. Without a tail surface it is possible, by careful placement of the *cg*, to use the weight-lift moment to balance the inherent negative pitching moment, but it is usually only possible to achieve a satisfactory arrangement for a limited range of operating conditions. A more flexible arrangement involves the use of special aerofoil sections with reflex camber toward the trailing edge, which can significantly reduce the magnitude of the section pitching moment.

Alternative arrangements are sometimes encountered in which trailing edge flaps are used to provide the reflex camber aerodynamics. Variable reflex camber is exploited to the limit in the hang glider, and pilot weight-lift moment is used to trim the pitching moment using weight shift control. A comprehensive analysis of the longitudinal static stability of the flexible tailless hang glider is given by Cook (1994). In more advanced-technology aircraft an easier solution is to utilise the advantages of command and stability augmentation systems to establish a stable controllable vehicle. However, in this case it remains a fundamental requirement that the longitudinal aerodynamic controls are capable of generating the longitudinal pitching moment for trim, stability augmentation, and control.

3.1.3 Degree of longitudinal stability

It was shown earlier that the condition for an aircraft to possess longitudinal static stability at a given trim condition is that the gradient of the $C_m - \alpha$ plot be negative. Obviously, a very large range of values of the gradient is possible, and the magnitude of the gradient determines the *degree of stability* possessed by the aircraft. Variation in the degree of longitudinal static stability is illustrated in Fig. 3.3. The degree of stability is described in terms of *stability margin*, which quantifies how much stability the aircraft has over and above zero or neutral stability. Thus, for example, the longitudinal static stability margin is directly related to the gradient of the $C_m - \alpha$ plot.

With reference to Fig. 3.3, and for a given disturbance in α, it is clear that the corresponding restoring pitching moment C_m is greatest for a very stable aircraft. The magnitude of the restoring moment decreases as the degree of stability, or stability margin, is reduced and becomes zero at neutral stability. When the aircraft is unstable the moment is clearly of the opposite sign and is therefore divergent. Thus the higher the degree of stability, the greater the restoring moment following a disturbance. This means that a very stable aircraft has significant pitch stiffness and will

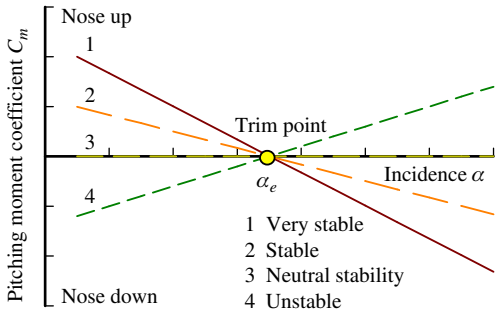

FIGURE 3.3 Degree of longitudinal static stability.

be very resistant to upset, which in turn means that greater control actions will be needed to encourage the aircraft to change its trim state or to manoeuvre. It follows, then, that the stability margins determine the magnitude of the control actions, quantified in terms of displacement and force, required to trim the aircraft. It is easy to appreciate that a consequence of this is that too much stability can be as hazardous as too little stability since the available control power is limited.

3.1.4 Variation in stability

Changes in the aerodynamic operating conditions of an aircraft which result in pitching moment changes inevitably lead to variation in longitudinal static stability. Such variation in stability is normally manifest as a nonlinear version of the C_m-C_L characteristic shown in Fig. 3.2. For the subsonic classical aircraft such changes are usually small and may result in some nonlinearity of the pitching moment characteristic with a change in trim. In general, the variation in the degree of stability is acceptably small. For the modern supersonic high-performance aircraft, the situation is not so well defined. Large flight envelopes and significant variation in flight condition can lead to dramatic changes in static stability. For example, it is possible for such an aircraft to be stable at some conditions and unstable at others. It easy to see how such variations might arise in a physical sense, but it is much more difficult to describe the variations in mathematical terms. A brief review of some of the more obvious sources of variation in stability follows.

Power effects

Probably the most significant variation in longitudinal static stability arises from the effects of power. Direct effects result from the point of application and line of action of the thrust forces with respect to the *cg*. Clearly, as illustrated in Fig. 3.4, a high thrust line results in a nose-down pitching moment and vice versa. In normal trimmed flight the thrust moment is additive to the aerodynamic moment, and the total pitching moment is trimmed to zero by adjustment of the elevator. However, any aerodynamic perturbation about trim which results in a thrust perturbation is potentially capable of giving rise to a nonlinear stability characteristic. The precise nature of the

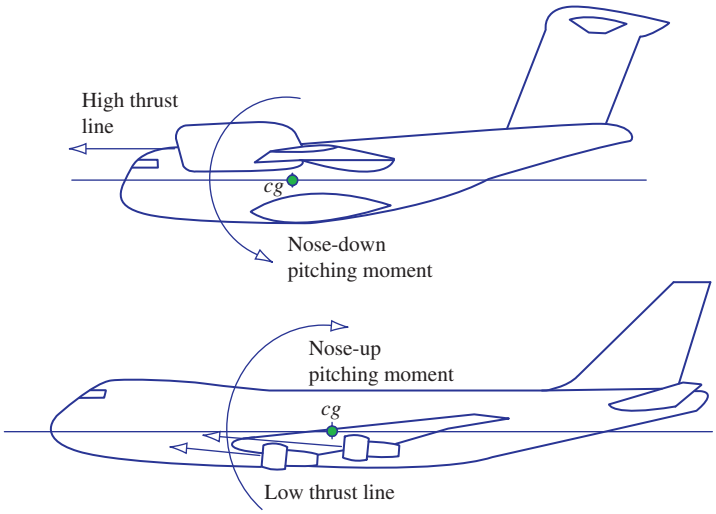

FIGURE 3.4 Typical thrust line effects on pitching moment.

variation in stability is dependent on the operating characteristics of the installed power unit, which may not be easy to identify.

Indirect power effects are caused by the induced flow associated with a propeller and its wake or the intake and exhaust of a gas turbine engine. Some of the more obvious induced-flow effects are illustrated in Fig. 3.5. The process of turning the incident flow through the body incidence angle into the propeller disc or into the engine intake creates a normal force at the propeller or engine intake as shown. In general, this effect gives rise to a nose-up pitching moment. The magnitude of the normal force is dependent on the body incidence angle and on the increase in flow energy at the propeller disc or engine intake. The force therefore varies considerably with trim condition. It is also sensitive to aerodynamic perturbations about trim, so it is easy to appreciate its contribution to pitching moment nonlinearity.

The wake behind a propeller is a region of high-energy flow, which modifies the aerodynamic operating conditions over parts of the wing and tailplane. The greatest effect on pitching moment arises from the tailplane. The effectiveness of the tailplane is enhanced simply because of increased flow velocity and reduced downwash angle. These two effects together increase the nose-down pitching moment available and hence increase the degree of stability of the aircraft. The induced-flow effects associated with propeller-driven aircraft can have a significant influence on longitudinal static stability. These effects also change with aerodynamic conditions, especially at high angles of attack. It is therefore quite common to see some nonlinearity in the pitching moment trim plot for such an aircraft at high values of lift coefficient. It should also be noted that the propeller wake rotates about the longitudinal axis. Although less significant, the rotating flow has some influence on the aircraft's lateral-directional static stability.

The exhaust from a jet engine, being a region of very high velocity and reduced pressure, creates an inflow field, as indicated in Fig. 3.5. Clearly, the influence on pitching moment depends on

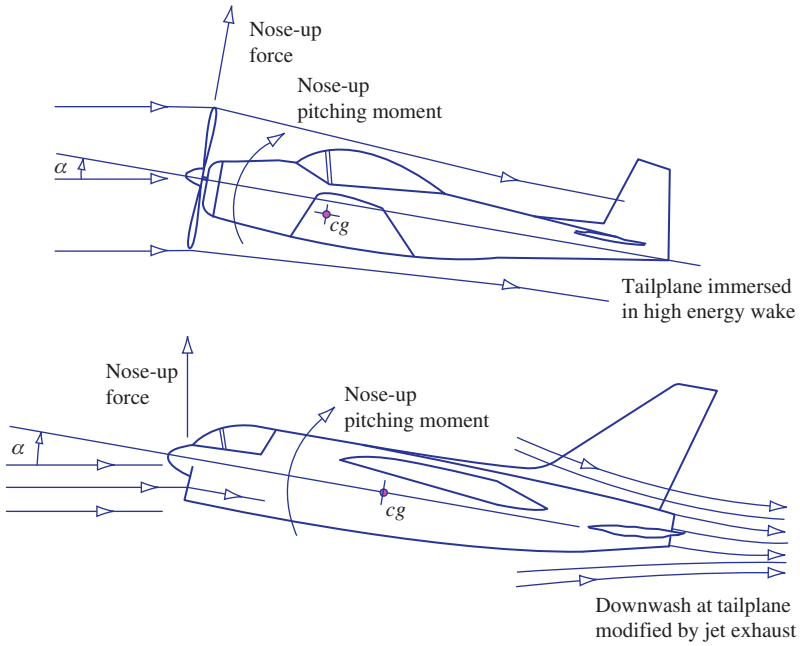

FIGURE 3.5 Typical induced-flow effects on pitching moment.

the relative location of the aerodynamic surfaces of the aircraft and the engine exhaust. When the tailplane is immersed in this induced-flow field, there is a change in the downwash angle. Thus the effect is to increase static stability when the downwash angle is reduced and vice versa. In general, this effect is not very significant, except perhaps for aircraft with engines mounted in pods on the rear fuselage and in which the tailplane is very close to the exhaust wake.

Other effects

Although power effects generally make the most significant contribution to variation in longitudinal static stability, other potentially important contributory sources also exist. For example, wing sweep back and aircraft geometry, which result in significant variation in downwash at the tailplane, generally tend to reduce the available stability, an effect which is clearly dependent on the aerodynamic trim condition. The fuselage alone is usually unstable, and the condition worsens with increasing Mach number. On the other hand, at high subsonic and supersonic Mach numbers the aerodynamic centres of the wing and tailplane move aft. This has the effect of increasing the available nose-down pitching moment, which is a stabilising characteristic. Finally, since all airframes have some degree of flexibility, the structure distorts under the influence of aerodynamic loads. Today aeroelastic distortion of the structure is carefully controlled by design and is not usually significant in influencing static stability. However, in very large civil transport aircraft the relative geometric disposition of the wing and tailplane changes with loading conditions; some contribution to the variation in pitching moment is therefore inevitable but is usually small.

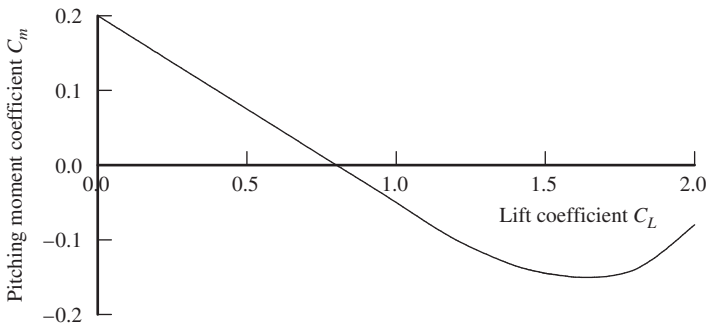

FIGURE 3.6 Stability reversal at a high lift coefficient.

Taking all of these effects together, the prospect of ever being able to quantitatively define the longitudinal static stability of an aircraft may seem daunting. Fortunately, these effects are well understood and can be minimised by design. The result for most aircraft is a pitching moment trim characteristic with some nonlinear tendency at higher values of trim lift coefficient. In extreme cases the stability of the aircraft can actually reverse at high values of lift coefficient, resulting in an unstable pitch-up characteristic. A typical pitching moment trim plot for an aircraft with a pitch-up characteristic is shown in Fig. 3.6.

EXAMPLE 3.1

To illustrate the variation in the pitching moment characteristic for a typical subsonic aircraft, the relevant data obtained from wind tunnel experiments on a 1/6th-scale model of the Handley Page HP-137 are plotted in Fig. 3.7. The data, extracted from a report by Storey (1966), were obtained at a tunnel speed of 200 ft/s, and the Reynolds number was $\mathrm{Re} = 1.2 \times 10^6$ based on mean aerodynamic chord $\bar{\bar{c}}$. The HP-137 is in fact the well-known Jetstream; however, it is not known if the data shown are representative of the actual aircraft flying today.

The plots show the characteristic for the aircraft without tail and for the aircraft with tail at various combinations of setting angle η_T and elevator angle η. Clearly, all of the plots are reasonably linear at all values of lift coefficient up to the stall. Without a tailplane the aircraft is unstable since the slope of the plot is positive. With tailplane the slope, and hence the degree of stability, is more or less constant. Assuming that the trim ($C_m = 0$) range of lift coefficient is approximately $-0.2 \leq C_L \leq 1.0$, by interpolation it can be seen that this can be obtained with an elevator angle range of approximately $-0.6^\circ \leq \eta \leq 0^\circ$. This is clearly well within the control capability of the tailplane and elevator configuration shown in this example.

This kind of experimental analysis is used to confirm the geometric design of the tailplane and elevator. In particular, it is essential to establish that the aircraft has an adequate stability margin across the trim envelope, that the elevator angle required to trim the aircraft is within its aerodynamic capability, and that a sufficient margin of elevator control range remains for manoeuvring.

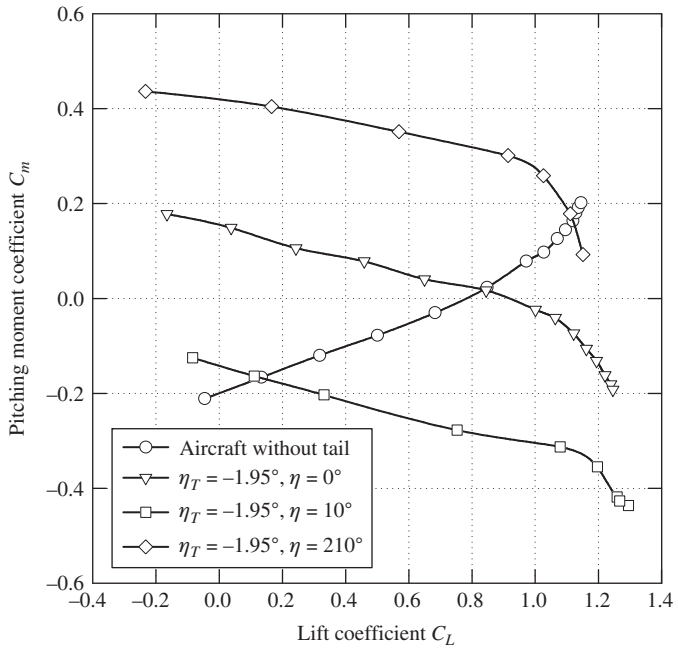

FIGURE 3.7 $C_m - \alpha$ **plots for a 1/6th scale model of the Handley Page Jetstream.**

3.2 The pitching moment equation

Having established the importance of pitching moment in the determination of longitudinal static stability, further analysis of stability requires the development of the pitching moment equation. A fully representative general pitching moment equation is difficult to develop since it is very dependent on the geometry of the aircraft. However, it is possible to develop a simple approximation which is sufficiently representative for most preliminary studies and which provides considerable insight into the basic requirements for static stability and trim.

3.2.1 Simple development of the pitching moment equation

For the development of the simplest possible pitching moment equation, it is usual to define a model showing only the normal forces and pitching moments acting on the aircraft. It is assumed that in steady level flight the thrust and drag are in equilibrium and act through the *cg*; it is further assumed that, for small disturbances in incidence, changes in this equilibrium are insignificant. These assumptions therefore imply that small disturbances in incidence cause significant changes in lift forces and pitching moments only. The model defined in these terms is shown in Fig. 3.8.

For the purposes of modelling pitching behaviour the model comprises two parts: the wing-fuselage combination and the tailplane. It is thus assumed that the wing-fuselage combination behave

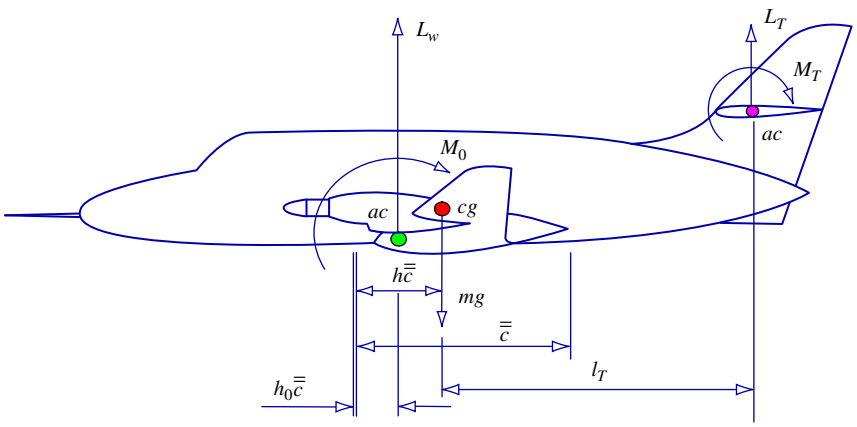

FIGURE 3.8 Simple pitching moment model.

aerodynamically like a wing alone. However, this is not strictly true since the fuselage may make significant aerodynamic contributions and, in any event, its presence interferes with the aerodynamic properties of the wing to a greater or lesser extent. However, for conventional subsonic aircraft with a wing of reasonably high aspect ratio this is a very satisfactory approximation. The tailplane is treated as a separate component since it provides the principal aerodynamic mechanism for controlling longitudinal static stability and trim. The following analysis establishes the fundamental importance of the tailplane parameters to longitudinal static stability.

Referring to Fig. 3.8, the wing-fuselage lift L_w and residual pitching moment M_0 act at the aerodynamic centre *ac* of the combination, which is assumed to be coincident with the aerodynamic centre of the wing alone. In a similar way the lift L_T and pitching moment M_T of the tailplane are assumed to act at its aerodynamic centre. The longitudinal geometry of the model is entirely related to the mean aerodynamic chord *mac* as shown in Fig. 3.8. An expression for the total pitching moment M about the *cg* may therefore be written as

$$M = M_0 + L_w(h - h_0)\bar{\bar{c}} - L_T l_T + M_T \tag{3.6}$$

If, as is usual, it is assumed that the tailplane aerofoil section is symmetric, then M_T becomes zero. Thus, in the more convenient coefficient form, equation (3.6) may be written as

$$C_m = C_{m_0} + C_{L_w}(h - h_0) - C_{L_T}\overline{V}_T \tag{3.7}$$

To facilitate further analysis of pitching moment it is necessary to express the tailplane lift coefficient C_{L_T} in terms of more accessible tailplane parameters. The tailplane lift coefficient may be expressed as

$$C_{L_T} = a_0 + a_1\alpha_T + a_2\eta + a_3\beta_\eta \tag{3.8}$$

where, a_0, a_1, a_2, and a_3 are constant aerodynamic coefficients, α_T is the local incidence, η is the elevator angle, and β_η is the elevator trim tab angle. Note that, since a symmetric tailplane aerofoil

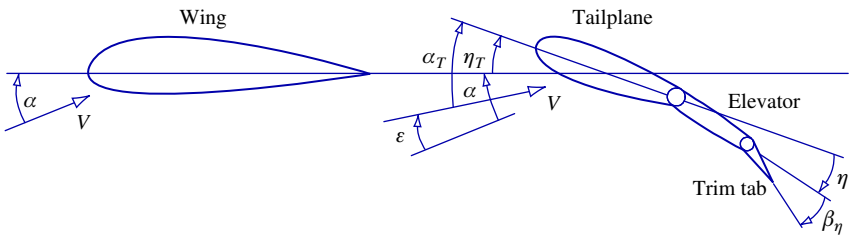

FIGURE 3.9 Wing-tailplane flow geometry.

section is assumed, a_0 is also zero. The local tailplane incidence is influenced by the *tailplane setting angle* η_T and the local flow distortion due to the effect of the downwash field behind the wing. The flow geometry is shown in Fig. 3.9.

Clearly, the angle of attack of the tailplane is given by

$$\alpha_T = \alpha - \varepsilon + \eta_T \tag{3.9}$$

where ε is the downwash angle at the tailplane. Since, to a good approximation, for small disturbances the downwash angle is a function of wing-body incidence α only,

$$\alpha - \varepsilon = \alpha\left(1 - \frac{\mathrm{d}\varepsilon}{\mathrm{d}\alpha}\right) = \frac{C_{L_w}}{a}\left(1 - \frac{\mathrm{d}\varepsilon}{\mathrm{d}\alpha}\right) \tag{3.10}$$

whence

$$\alpha_T = \frac{C_{L_w}}{a}\left(1 - \frac{\mathrm{d}\varepsilon}{\mathrm{d}\alpha}\right) + \eta_T \tag{3.11}$$

Now, substituting the expression for α_T given by equation (3.11) into equation (3.8), substituting the resulting expression for C_{L_T} into equation (3.7), and noting that a_0 is zero, the pitching moment equation in its simplest and most general form is obtained:

$$C_m = C_{m_0} + C_{L_w}(h - h_0) - \overline{V}_T\left(C_{L_w}\frac{a_1}{a}\left(1 - \frac{\mathrm{d}\varepsilon}{\mathrm{d}\alpha}\right) + a_2\eta + a_3\beta_\eta + a_1\eta_T\right) \tag{3.12}$$

A simple computational algorithm for estimating the rate of change in downwash with angle of attack $\mathrm{d}\varepsilon/\mathrm{d}\alpha$ is given in Stribling (1984) and its use is illustrated in the Mathcad trim program listed in Appendix 1.

3.2.2 Elevator angle to trim

It has already been shown, in equation (3.1), that the condition for trim is that the total pitching moment be adjustable to zero (i.e., $C_m = 0$). Applying this condition to equation (3.12), the elevator angle required to trim the aircraft is given by

$$\eta = \frac{1}{\overline{V}_T a_2}(C_{m_0} + C_{L_w}(h - h_0)) - \frac{C_{L_w}}{a}\left(\frac{a_1}{a_2}\right)\left(1 - \frac{\mathrm{d}\varepsilon}{\mathrm{d}\alpha}\right) - \frac{a_3}{a_2}\beta_\eta - \frac{a_1}{a_2}\eta_T \tag{3.13}$$

When the elevator tab is set at its neutral position, $\beta_\eta = 0$, and for a given *cg* position h, the elevator angle to trim varies only with lift coefficient. For any other tab setting a different elevator angle is required to trim. Therefore, the elevator and elevator tab to an extent provide interchangeable means for achieving longitudinal trim.

3.2.3 Condition for longitudinal static stability

The basic requirement for an aircraft to be statically stable at a given trim condition is stated in equation (3.2). By differentiating equation (3.12) with respect to C_L or, equivalently, C_{L_w}, and noting that η_T and, by definition, C_{m_0}, are constants, the condition for the aircraft to be stable is given by

$$\frac{\mathrm{d}C_m}{\mathrm{d}C_{L_w}} < 0$$

where

$$\frac{\mathrm{d}C_m}{\mathrm{d}C_{L_w}} = (h - h_0) - \overline{V}_T \left(\frac{a_1}{a} \left(1 - \frac{\mathrm{d}\varepsilon}{\mathrm{d}\alpha} \right) + a_2 \frac{\mathrm{d}\eta}{\mathrm{d}C_{L_w}} + a_3 \frac{\mathrm{d}\beta_\eta}{\mathrm{d}C_{L_w}} \right) \tag{3.14}$$

Thus, at a given *cg* position h, the longitudinal static stability of the aircraft and the aerodynamic control characteristics—that is, *elevator angle to trim*, $\mathrm{d}\eta/\mathrm{d}C_{l_w}$, and *elevator tab angle to trim*, $\mathrm{d}\beta_\eta/\mathrm{d}C_{L_w}$—are interdependent. Further analysis is usually carried out by separating the effects of elevator angle and tab angle in equation (3.14). *Controls-fixed stability* is concerned with the interdependence of elevator angle to trim and stability, whereas *controls-free stability* is concerned with the interdependence of elevator tab angle to trim and stability.

3.3 Longitudinal static stability

A more detailed analysis of longitudinal static stability leads to a description of pilot control actions to trim. In particular, control displacement is determined by controls-fixed stability and control force to trim is determined by controls-free stability.

3.3.1 Controls-fixed stability

The condition described as *controls-fixed* is taken to mean the condition when the elevator and elevator tab are held at constant settings corresponding to the prevailing trim condition. In practice, this means that the pilot is flying the aircraft with his hands on the controls and is holding the controls at the *fixed* setting required to trim. This, of course, assumes that the aircraft is stable and remains in trim.

Since the controls are fixed,

$$\frac{\mathrm{d}\eta}{\mathrm{d}C_{L_w}} = \frac{\mathrm{d}\beta_\eta}{\mathrm{d}C_{L_w}} = 0 \tag{3.15}$$

and equation (3.14) may be written as

$$\frac{\mathrm{d}C_m}{\mathrm{d}C_{L_w}} = (h - h_0) - \overline{V}_T \frac{a_1}{a} \left(1 - \frac{\mathrm{d}\varepsilon}{\mathrm{d}\alpha} \right) \tag{3.16}$$

or as

$$K_n = -\frac{dC_m}{dC_{L_w}} = h_n - h \tag{3.17}$$

where K_n is the *controls-fixed stability margin*, the slope of the $C_m - C_L$ plot. The location of the *controls-fixed neutral point* h_n on the mean aerodynamic chord $\bar{\bar{c}}$ is therefore given by

$$h_n = h_0 + \overline{V}_T \frac{a_1}{a}\left(1 - \frac{d\varepsilon}{d\alpha}\right) \tag{3.18}$$

For a statically stable aircraft the stability margin K_n is positive, and the greater its value the greater the degree of stability. With reference to equation (3.17), it is clear that the aircraft is stable when the *cg* position h is ahead of the controls-fixed neutral point h_n. The acceptable margins of stability therefore determine the permitted range of *cg* position in a given aircraft. The aft limit often corresponds with the controls-fixed neutral point, whereas the forward limit is determined by the maximum permissible stability margin. Recall from Section 3.1.3 that too much stability can be as hazardous as too little.

The meaning of controls-fixed stability is easily interpreted by considering the pilot actions required to trim an aircraft in a controls-fixed sense. It is assumed at the outset that the aircraft is in fact stable and hence can be trimmed to an equilibrium flight condition. When the aircraft is in a trimmed initial equilibrium state the pitching moment is zero and equation (3.12) may be written as

$$0 = C_{m_0} + C_{L_w}(h - h_0) - \overline{V}_T\left(C_{L_w}\frac{a_1}{a}\left(1 - \frac{d\varepsilon}{d\alpha}\right) + a_2\eta + a_3\beta_\eta + a_1\eta_T\right) \tag{3.19}$$

It is assumed that the pilot is holding the controls at the required elevator angle, the power is set to give steady level flight, and the elevator tab is set at its datum, $\beta_\eta = 0$. Now, to retrim the aircraft at a new flight condition in a controls-fixed sense it is necessary for the pilot to move the controls to the new elevator setting and then to hold the controls at that setting. For example, to retrim at a higher speed in a more nose-down attitude, the pilot moves the control column forward until his new condition is established and then to simply hold the column at that position. This of course leaves the aircraft in a descending condition unless the power is increased sufficient to maintain level flight at the higher speed. However, power variations are not allowed for in the simple model reviewed here.

Thus trimming a stable aircraft at any condition in its speed envelope simply requires the selection of the correct elevator angle, all other parameters remaining constant. The variable in controls-fixed stability analysis is therefore elevator angle to trim. Differentiating equation (3.19) with respect to C_{L_w} and making the same assumptions as before, but allowing elevator angle η to vary with trim, it may be shown, after some rearrangement, that

$$\frac{d\eta}{dC_{L_w}} = \frac{-1}{\overline{V}_T a_2}(h_n - h) = \frac{-1}{\overline{V}_T a_2} K_n \tag{3.20}$$

Since $\overline{V}_T$ and a_2 are constants, the *elevator angle to trim* characteristic $d\eta/dC_{L_w}$ is thus proportional to the controls-fixed stability margin K_n. Measurements of elevator angle to trim for a range of flight conditions, subject to the assumptions described, provide a practical means for determining

controls-fixed stability characteristics from flight experiments. However, in such experiments it is not generally possible to completely eliminate the effects of power on the results.

EXAMPLE 3.2

The practical evaluation of controls-fixed static stability centres on the application of equations (3.13), (3.19), and (3.20) to a stable aircraft. It is relatively straightforward to obtain measurements of the elevator angle η required to trim an aircraft at a chosen value of lift coefficient C_L. Provided that the power and elevator trim tab angle β_η are maintained at constant settings throughout the measurement process, the equations apply directly. A flight test exercise conducted in a Handley Page Jetstream by the author under these conditions provided the trim data plotted in Fig. 3.10 for three different *cg* positions. At any given value of lift coefficient C_L the corresponding value of elevator angle to trim η is given by the solution of equation (3.13) or, alternatively, equation (3.19). The plots are clearly nonlinear and the nonlinearity in this aircraft is almost entirely due to the effects of power.

Since the gradients of the plots shown in Fig. 3.10 are all negative, the aircraft is statically stable in accordance with equation (3.20). However, for any given *cg* position the gradient varies with lift coefficient, indicating a small variation in stability margin. In a detailed analysis the stability margin would be evaluated at each value of trimmed lift coefficient in order to quantify

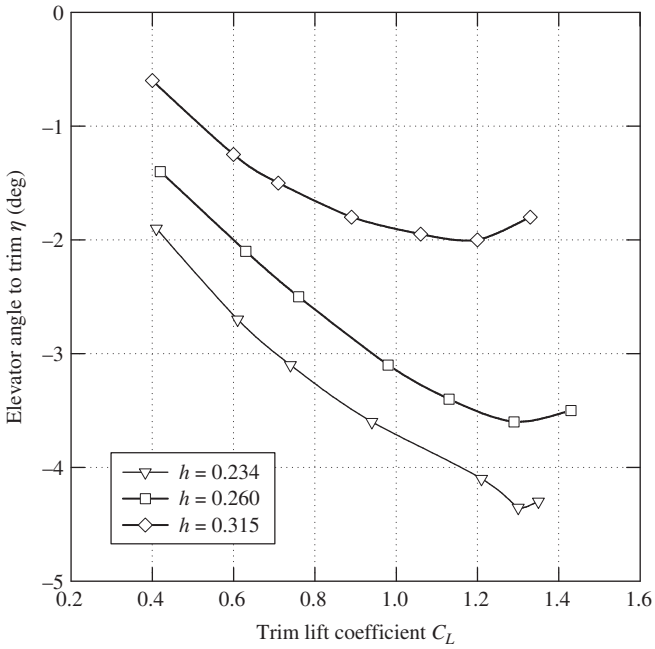

FIGURE 3.10 Plot of elevator angle to trim.

the variation in stability. In the present example the quality of the data was not good enough to allow such a complete analysis. To establish the location of the controls-fixed neutral point h_n, equation (3.20) must be solved at each value of trim lift coefficient. This is most easily done graphically, as shown in Fig. 3.11.

Equation (3.20) is solved by plotting $d\eta/dC_L$ against *cg* position h as shown. In this example the mean gradient for each *cg* position, rather than the value at each trim point, is plotted. Since equation (3.20) represents a linear plot, a straight line may be fitted to the three data points as shown. Extrapolation to the neutral stability point at which $d\eta/dC_L = 0$ corresponds with a *cg* position of approximately $h = 0.37$. Clearly, three data points through which to draw a line is barely adequate for this kind of evaluation. A controls-fixed neutral point h_n at 37% of *mac* correlates well with the known properties of the aircraft. The most aft *cg* position permitted is in fact at 37% of *mac*. With the location of the controls-fixed neutral point established, the controls-fixed stability margin K_n for each *cg* position follows from the application of equation (3.20).

In a more searching stability evaluation, rather more data points would be required and data of much better quality would be essential. Although limited, the present example does illustrate the typical controls-fixed longitudinal static stability characteristics of a well-behaved classical aircraft.

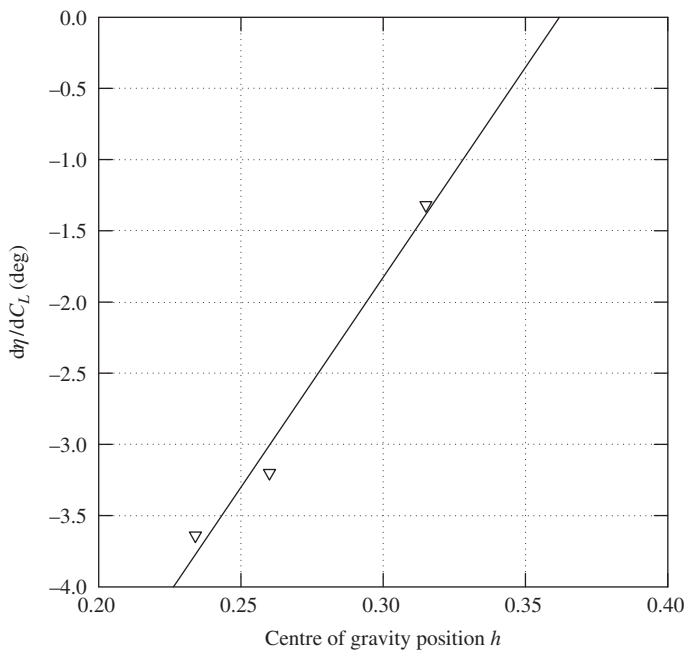

FIGURE 3.11 Determination of controls-fixed neutral point.

3.3.2 Controls-free stability

The condition described as *controls-free* is taken to mean the condition when the elevator is free to float at an angle corresponding to the prevailing trim condition. In practice this means that the pilot can fly the aircraft with his hands off the controls whilst the aircraft remains in its trimmed flight condition. Again, it is assumed that the aircraft is stable; otherwise, it would diverge when the controls were released. Now this situation can only be obtained if the controls can be adjusted such that the elevator floats at the correct angle for the desired *hands-off* trim condition. This is arranged by adjusting the elevator trim tab until the required trim is obtained. Thus controls-free stability is concerned with the trim tab and its control characteristics.

When the controls are free, the elevator hinge moment H is zero and the elevator floats at an indeterminate angle η. It is therefore necessary to eliminate elevator angle from the pitching moment equation (3.12) in order to facilitate analysis of controls-free stability. The elevator hinge moment coefficient is given by the expression

$$C_H = b_1\alpha_T + b_2\eta + b_3\beta_\eta \tag{3.21}$$

where, b_1, b_2, and b_3 are constants determined by the design of the elevator and trim tab control circuitry. Substituting for local tailplane incidence α_T as given by equation (3.11), equation (3.21) may be rearranged to determine the angle at which the elevator floats. Thus

$$\eta = \frac{1}{b_2}C_H - \frac{C_{L_w}}{a}\frac{b_1}{b_2}\left(1 - \frac{\mathrm{d}\varepsilon}{\mathrm{d}\alpha}\right) - \frac{b_3}{b_2}\beta_\eta - \frac{b_1}{b_2}\eta_T \tag{3.22}$$

To eliminate elevator angle from the pitching moment equation, substitute equation (3.22) into equation (3.12) to obtain

$$C_m = C_{m_0} + C_{L_w}(h - h_0) - \overline{V}_T\left(\begin{array}{l} C_{L_w}\dfrac{a_1}{a}\left(1 - \dfrac{\mathrm{d}\varepsilon}{\mathrm{d}\alpha}\right)\left(1 - \dfrac{a_2b_1}{a_1b_2}\right) + a_3\beta_\eta\left(1 - \dfrac{a_2b_3}{a_3b_2}\right) \\ + a_1\eta_T\left(1 - \dfrac{a_2b_1}{a_1b_2}\right) + \dfrac{a_2}{b_2}C_H \end{array}\right) \tag{3.23}$$

Now, in the controls-free condition $C_H = 0$, and noting that η_T, C_{m_0} and, since the tab is set at the trim value, β_η are constants, differentiating equation (3.23) with respect to C_{L_w} gives

$$\frac{\mathrm{d}C_m}{\mathrm{d}C_{L_w}} = (h - h_0) - \overline{V}_T\frac{a_1}{a}\left(1 - \frac{\mathrm{d}\varepsilon}{\mathrm{d}\alpha}\right)\left(1 - \frac{a_2b_1}{a_1b_2}\right) \tag{3.24}$$

Or, writing,

$$K'_n = -\frac{\mathrm{d}C_m}{\mathrm{d}C_{L_w}} = h'_n - h \tag{3.25}$$

where K'_n is the *controls-free stability margin*, the slope of the C_m–C_L plot with the controls free. The location of the *controls-free neutral point* h'_n on the mean aerodynamic chord $\bar{\bar{c}}$ is given by

$$\begin{aligned} h'_n &= h_0 + \overline{V}_T \frac{a_1}{a}\left(1 - \frac{\mathrm{d}\varepsilon}{\mathrm{d}\alpha}\right)\left(1 - \frac{a_2 b_1}{a_1 b_2}\right) \\ &= h_n - \overline{V}_T \frac{a_2 b_1}{a b_2}\left(1 - \frac{\mathrm{d}\varepsilon}{\mathrm{d}\alpha}\right) \end{aligned} \tag{3.26}$$

As before, for a statically stable aircraft the controls-free stability margin K'_n is positive and the greater its value, the greater the degree of stability possessed by the aircraft. With reference to equation (3.25), it is clear that for controls-free stability the *cg* position h must be ahead of the controls-free neutral point h'_n. Equation (3.26) shows the relationship between the controls-fixed and controls-free neutral points. The numerical values of the elevator and tab constants are such that usually $h'_n > h_n$, which means that it is common for the controls-free neutral point to lie aft of the controls-fixed neutral point. Thus an aircraft that is stable controls-fixed is also usually stable controls-free, and it follows that the controls-free stability margin K'_n is greater than the controls-fixed stability margin K_n.

The meaning of controls-free stability is readily interpreted by considering the pilot actions required to trim the aircraft in a controls-free sense. It is assumed that the aircraft is stable and is initially in a hands-off trim condition. In this condition the pitching moment is zero and hence equation (3.23) may be written as

$$0 = C_{m_0} + C_{L_w}(h - h_0) - \overline{V}_T \left(\begin{array}{l} C_{L_w} \dfrac{a_1}{a}\left(1 - \dfrac{\mathrm{d}\varepsilon}{\mathrm{d}\alpha}\right)\left(1 - \dfrac{a_2 b_1}{a_1 b_2}\right) \\ + a_3 \beta_\eta \left(1 - \dfrac{a_2 b_3}{a_3 b_2}\right) + a_1 \eta_T \left(1 - \dfrac{a_2 b_1}{a_1 b_2}\right) \end{array} \right) \tag{3.27}$$

To retrim the aircraft it is necessary for the pilot to grasp the control column and move it to the position corresponding with the elevator angle required for the new trim condition. However, if he releases the control it will simply move back to its original trim position since an out-of-trim elevator hinge moment, and hence stick force, exists at the new position. To rectify the problem the pilot must use the trim tab. Having moved the control to the position corresponding with the new trim condition, he will be holding a force on the control. By adjusting the trim tab he can null the force and following which, he can release the control and it will remain in the new hands-off position as required. Thus trim tab adjustment is equivalent to control force adjustment, which in turn is directly related to elevator hinge moment adjustment in a mechanical flying control system.

To reiterate the previous illustration, consider the situation when the pilot wishes to retrim the aircraft at a higher speed in a more nose-down attitude. As before, he will *push* the control column forward until the desired condition is obtained, which will leave him holding an out-of-trim force and descending. Elevator tab adjustment will enable him to reduce the control force to zero, whereupon the pilot can release the control to enjoy his new hands-off trim condition. Since he is descending it is normally necessary to increase power in order to regain level flight. However, as already stated, thrust variations are not allowed in this model; if they were, the analysis would be considerably more complex.

Thus to trim a stable aircraft at any hands-off flight condition in its speed envelope simply requires the correct selection of elevator tab angle. The variable in controls-free stability analysis is therefore elevator tab angle to trim. Differentiating equation (3.27) with respect to C_{L_w} and making the same assumptions as previously but allowing elevator tab angle β_η to vary with trim, after some rearrangement it may be shown that

$$\frac{\mathrm{d}\beta_\eta}{\mathrm{d}C_{L_w}} = \frac{-(h'_n - h)}{a_3\overline{V}_T\left(1 - \dfrac{a_2 b_3}{a_3 b_2}\right)} = \frac{-K'_n}{a_3\overline{V}_T\left(1 - \dfrac{a_2 b_3}{a_3 b_2}\right)} \tag{3.28}$$

Since it is usual for

$$-a_3\overline{V}_T\left(1 - \frac{a_2 b_3}{a_3 b_2}\right) > 0 \tag{3.29}$$

the *elevator tab angle to trim* characteristic $\mathrm{d}\beta_\eta/\mathrm{d}C_{L_w}$ is positive and proportional to the controls-free stability margin K'_n. Measurement of the tab angles required to trim a range of flight conditions, subject to the assumptions described, provides a practical means for determining controls-free stability characteristics from flight experiments. However, since tab angle, elevator hinge moment, and control force are all equivalent, it is often more meaningful to investigate control force to trim directly since this is the parameter of direct concern to the pilot.

To determine the equivalence between elevator tab angle to trim and control force to trim, consider the aircraft in a stable hands-off trim state with the tab set at its correct trim value. If the pilot moves the controls in this condition, the elevator hinge moment, and hence control force, will vary. Equation (3.23) is applicable and may be written as

$$0 = C_{m_0} + C_{L_w}(h - h_0) - \overline{V}_T\left(\begin{array}{l} C_{L_w}\dfrac{a_1}{a}\left(1 - \dfrac{\mathrm{d}\varepsilon}{\mathrm{d}\alpha}\right)\left(1 - \dfrac{a_2 b_1}{a_1 b_2}\right) + a_3\beta_\eta\left(1 - \dfrac{a_2 b_3}{a_3 b_2}\right) \\ \quad + a_1\eta_T\left(1 - \dfrac{a_2 b_1}{a_1 b_2}\right) + \dfrac{a_2}{b_2}C_H \end{array}\right) \tag{3.30}$$

where β_η is set at its datum trim position and is assumed constant, and hinge moment coefficient C_H is allowed to vary with trim condition. Differentiate equation (3.30) with respect to C_{L_w} subject to these conditions, and rearrange to obtain

$$\frac{\mathrm{d}C_H}{\mathrm{d}C_{L_w}} = \frac{-1}{\overline{V}_T\dfrac{a_2}{b_2}}(h'_n - h) = \frac{-1}{\overline{V}_T\dfrac{a_2}{b_2}}K'_n \tag{3.31}$$

Comparison of equation (3.31) with equation (3.28) demonstrates the equivalence of tab angle to trim and hinge moment to trim. Further, if the elevator control force is denoted F_η and g_η denotes the mechanical gearing between the control column and elevator, then

$$F_\eta = g_\eta H = \frac{1}{2}\rho V_0^2 S_\eta \overline{\overline{c}}_\eta g_\eta C_H \tag{3.32}$$

where S_η is the elevator area aft of the hinge line and $\overline{\overline{c}}_\eta$ is the mean aerodynamic chord of the elevator aft of the hinge line. This therefore demonstrates the relationship between control force and hinge moment, although equation (3.32) shows that the relationship also depends on the square of the speed.

EXAMPLE 3.3

The practical evaluation of controls-free static stability is undertaken in much the same way as the evaluation of controls-fixed stability discussed in Example 3.2. In this case the evaluation centres on the application of equations (3.30), (3.31), and (3.32) to a stable aircraft. It is relatively straightforward to obtain measurements of the elevator stick force F_η, and hence the hinge moment coefficient C_H, required to trim an aircraft at a chosen value of lift coefficient C_L. Provided that the power and elevator trim tab angle β_η are maintained at constant settings throughout the measurement process, the above mentioned equations apply directly.

As before, a flight test exercise conducted in a Handley Page Jetstream under these conditions provided the trim data plotted in Fig. 3.12 for three different cg positions. At any given value of lift coefficient C_L, the corresponding value of elevator hinge moment to trim C_H is given by the solution of equation (3.30). Again, the plots are nonlinear primarily because of the effects of

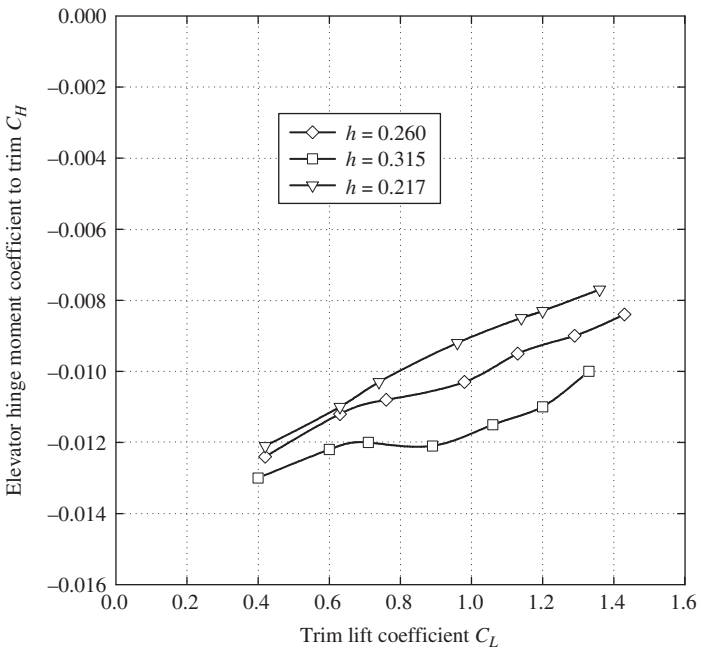

FIGURE 3.12 Plot of hinge moment coefficient to trim.

power. However, since force measurements are involved, the influence of friction in the mechanical control runs is significant and inconsistent. The result of this is data with rather too many spurious points. To provide a meaningful example, the obviously spurious data points have been "adjusted" to correlate with the known characteristics of the aircraft.

Since the gradients of the plots shown in Fig. 3.12 are all positive, the aircraft is statically stable in accordance with equation (3.31). However, for any given *cg* position the gradient varies with lift coefficient, indicating rather inconsistent variations in stability margin. However, in this case the variations are more likely to be the result of poor-quality data rather than orderly changes in the aerodynamic properties of the aircraft. Again, in a detailed analysis the stability margin would be evaluated at each value of trimmed lift coefficient in order to quantify the variation in stability. In the present example the data were clearly not good enough to allow such a complete analysis. To establish the location of the controls-free neutral point h_n', equation (3.31) must be solved at each value of trim lift coefficient. This is most easily done graphically as shown in Fig. 3.13.

Equation (3.31) is solved by plotting $\mathrm{d}C_H/\mathrm{d}C_L$ against *cg* position h as shown. In this example the mean gradient for each *cg* position is plotted rather than the value at each trim point. Since equation (3.31) represents a linear plot, a straight line may be fitted to the three data points as

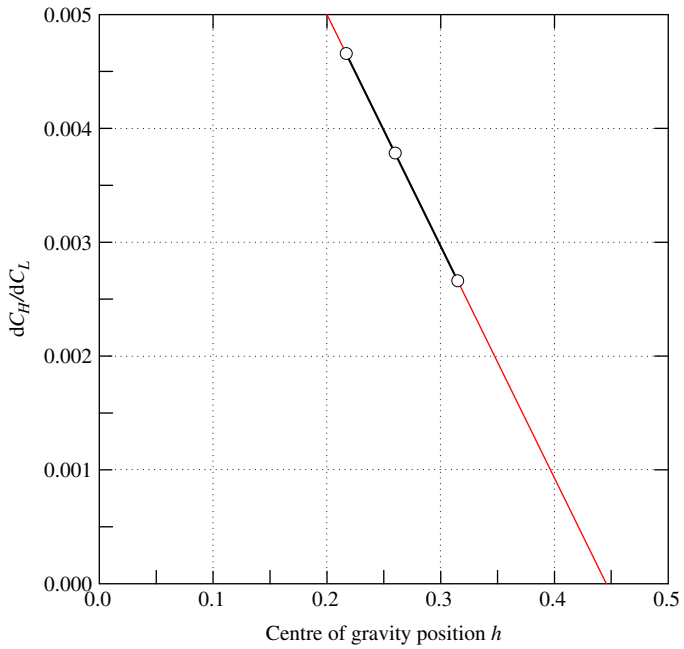

FIGURE 3.13 Determination of the controls-free neutral point.

shown. Extrapolation to the neutral stability point at which $dC_H/dC_L = 0$ corresponds with a *cg* position of approximately $h = 0.44$. A controls-free neutral point h'_n at 44% of *mac* correlates reasonably well with the known properties of the aircraft. Having established the location of the controls-free neutral point, the controls-free stability margin K'_n for each *cg* position follows from the application of equation (3.25).

3.3.3 Summary of longitudinal static stability

A physical interpretation of the meaning of longitudinal static stability may be brought together in the summary shown in Fig. 3.14. The important parameters are neutral point positions and their relationship to the *cg* position, which in turn determines the stability margins of the aircraft. The stability margins determine literally how much stability the aircraft has in hand, in the controls-fixed and controls-free senses, over and above neutral stability. The margins therefore indicate how safe the aircraft is. Equally important, however, the stability margins provide a measure of the control actions required to trim the aircraft. In particular, the controls-fixed stability margin is a measure of the control displacement required to trim and the controls-free stability margin is a measure of the control force required to trim.

From a flying and handling qualities point of view, it is the interpretation of stability in terms of control characteristics which is by far the most important consideration. In practice, the assessment of longitudinal static stability is frequently concerned only with the measurement of control characteristics, as illustrated by Examples 3.2 and 3.3.

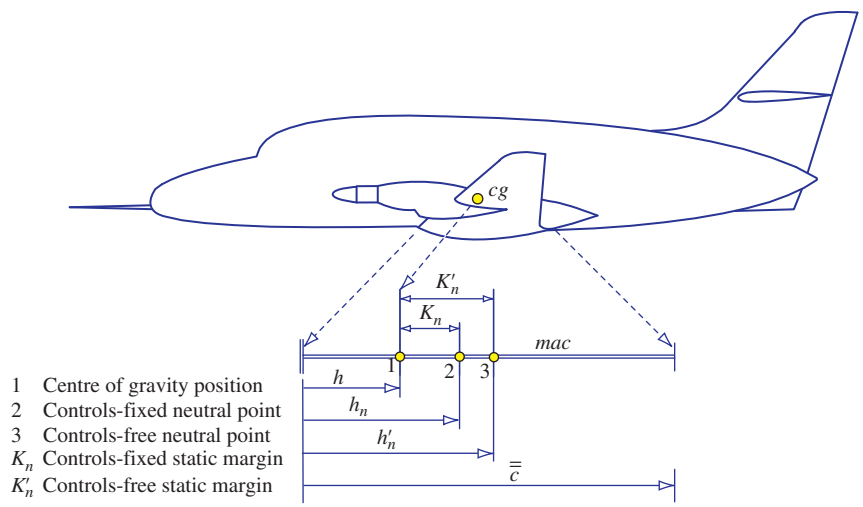

FIGURE 3.14 Longitudinal stability margins.

3.4 Lateral-directional static stability

Lateral-directional static stability is concerned with the ability of the aircraft to recover equilibrium following a sideslip disturbance; it is the lateral-directional equivalent to longitudinal static stability in its interpretation. As discussed in Section 3.1.1, the lateral-directional equilibrium trim state is determined by the condition when the net side force and the net roll and yaw moments are all zero. Since conventional aircraft are geometrically symmetric, the side force is zero in trimmed rectilinear flight; whenever the aircraft experiences a sideslip disturbance, the resulting out-of-trim side force always acts in a sense to oppose the disturbance. Such a condition is always stable, so the lateral-directional stability properties of the aircraft reduce to a consideration of roll and yaw moment response to a sideslip disturbance. As for longitudinal stability, the transient motion following such a disturbance is characterised by the dynamic stability properties, and the stable aircraft will eventually settle to its equilibrium state once more.

A positive sideslip disturbance is shown in Fig. 3.15, in which the aircraft slips to the right with velocity v. Thus the disturbed aircraft velocity vector V is displaced to the right through the sideslip angle β, and it is easily determined that

$$\tan\beta = \frac{v}{U} \tag{3.33}$$

where U is the axial component of velocity in the disturbance. Since the disturbance is assumed to be small, and in reality a sideslip angle greater than 10° would be considered excessive, it is usual to write

$$\beta \cong \frac{v}{U} \cong \frac{v}{V_0} \tag{3.34}$$

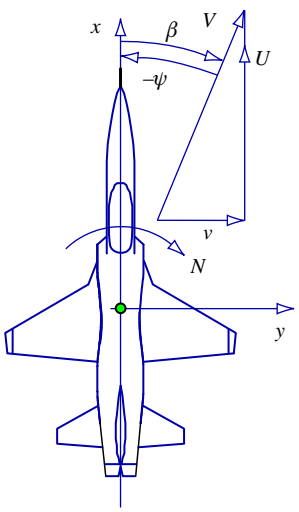

FIGURE 3.15 Sideslip disturbance.

where V_0 is the undisturbed equilibrium velocity of the aircraft. As shown in Fig. 3.15, in the disturbance the nose of the aircraft is displaced to the left of the velocity vector and the sideslip angle β is equivalent to the yaw angle $-\psi$ since the disturbance is assumed small.

Because the lateral-directional static stability of the aircraft is usually fixed by design, it usually remains more or less constant throughout the flight envelope. The lateral-directional stability margins therefore remain nominally constant for all flight conditions. This situation may well break down when large-amplitude manoeuvring is considered. Under such circumstances normally linear aerodynamic behaviour may well become very nonlinear and cause dramatic changes to observed lateral-directional stability and control characteristics. Although of considerable interest to the flight dynamicist, nonlinear behaviour is beyond the scope of this book. Nominally constant lateral-directional static stability is assumed throughout.

In general, the degree of lateral-directional static stability is quantified by the aerodynamic stability derivatives L_v and N_v or, equivalently, L_β and N_β, and a full analytical derivation and discussion of the derivatives is given in Section 13.3.2.

3.4.1 Lateral static stability

Lateral static stability is concerned with the ability of the aircraft to maintain wings-level equilibrium in the roll sense. Wing dihedral is the most visible parameter which confers lateral static stability on an aircraft, although there are many other contributions, some of which are destabilising. Since all aircraft are required to fly with their wings level in the steady trim state, lateral static stability is designed in from the outset. Dihedral is the easiest parameter to adjust in the design process in order to "tune" the degree of stability to an acceptable level. Remember that too much lateral static stability results in an aircraft that is reluctant to manoeuvre in roll, so it is important to obtain the correct degree of stability in order not to compromise aileron control power. A more detailed analysis of lateral control derivatives is given in Section 13.4.2.

The effect of dihedral as a means for providing lateral static stability is easily appreciated by considering the situation depicted in Fig. 3.16. Following a small positive disturbance in sideslip β, the right wing tends to drop and the aircraft slides "downhill" to the right with a sideslip velocity v. Consider the resulting change in the aerodynamic conditions on the leading right wing, which has dihedral angle Γ. Since the wing has dihedral, the sideslip velocity has a small component v' resolved perpendicular to the plane of the wing panel. where

$$v' = v \sin\Gamma \tag{3.35}$$

The velocity component v' combines with the axial velocity component U_e to increase the angle of attack of the leading wing by α'. Since $v' << U_e$, the change in angle of attack α' is small and the total disturbed axial velocity component $U \cong U_e$. The increase in angle of attack on the leading wing gives rise to an increase in lift, which in turn gives rise to a restoring rolling moment $-L$. The corresponding aerodynamic change on the left wing trailing into the sideslip results in a small decrease in lift, which also produces a restoring rolling moment. The net effect is therefore to create a negative rolling moment which causes the aircraft to recover its zero sideslip wings-level

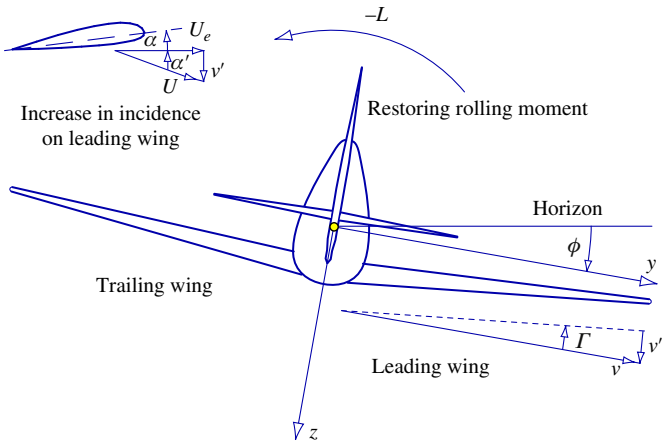

FIGURE 3.16 Dihedral effect.

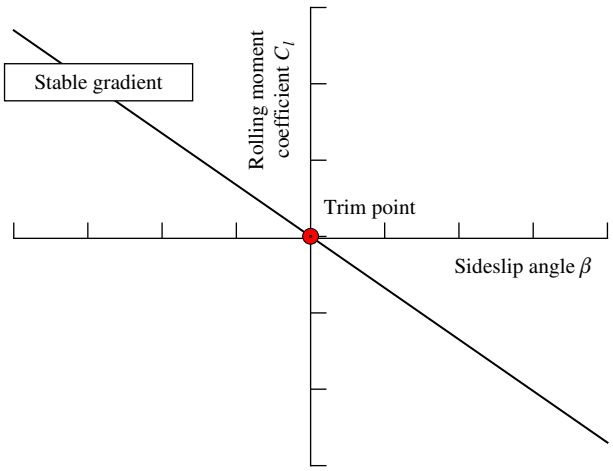

FIGURE 3.17 $C_l - \beta$ plot for a stable aircraft.

equilibrium. Thus the condition for an aircraft to be laterally stable is that the rolling moment resulting from a positive disturbance in sideslip be negative, or, in mathematical terms,

$$\frac{\mathrm{d}C_l}{\mathrm{d}\beta} < 0 \tag{3.36}$$

where C_l is the rolling moment coefficient. This is shown graphically in Fig. 3.17 and may be interpreted in a similar way to the pitching moment plot shown in Fig. 3.2.

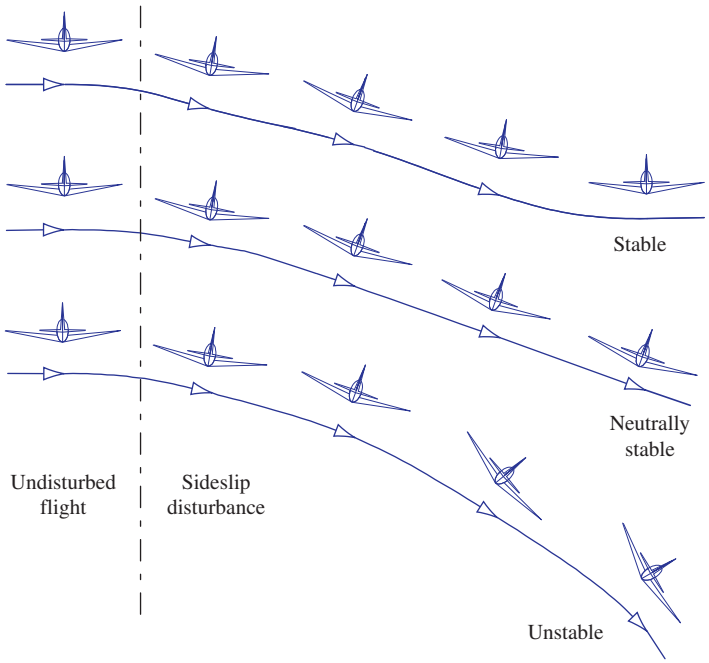

FIGURE 3.18 Effect of dihedral on lateral stability.

Note that the trim point for all flight conditions corresponds with zero sideslip angle, and that the gradient of the rolling moment against sideslip plot must be negative for stability. As in the case of longitudinal static stability, the magnitude of the gradient determines the degree of lateral static stability; the correct value provides a satisfactory balance between stability and roll control of the aircraft.

The sequence of events following a sideslip disturbance are shown for a laterally stable, neutrally stable, and unstable aircraft in Fig. 3.18. However, it must be remembered that, once disturbed, the subsequent motion will be determined by the lateral dynamic stability characteristics as well.

Wing sweep can also make a significant positive contribution to lateral static stability. For this reason dihedral is not commonly seen on swept-wing combat aircraft in order to avoid an excessive level of lateral stability, which would compromise roll manoeuvre performance. Indeed, anhedral (negative dihedral), which is destabilising, is used on some swept-wing combat aircraft as a means of "tuning" lateral static stability to an acceptable level.

With reference to Fig. 3.15, a wing in sideslip is effectively yawed through the sideslip angle such that $\psi = -\beta$. A swept wing in sideslip is therefore treated as a yawed wing, and it must be remembered that the disturbed aircraft tends to roll in the direction of sideslip. Now the lift on a

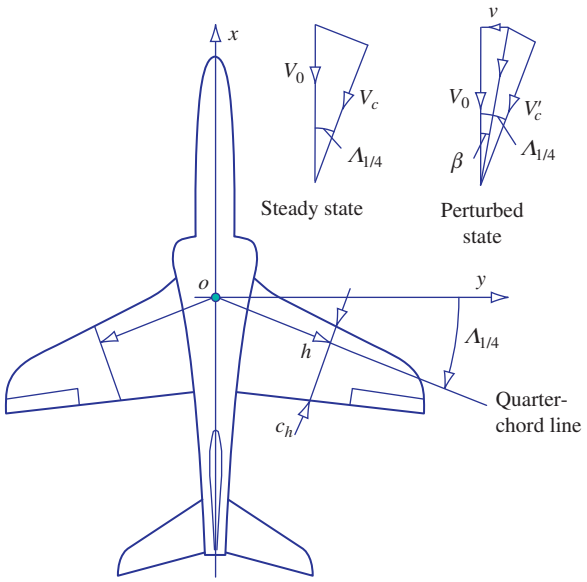

FIGURE 3.19 Swept wing in sideslip.

yawed wing is determined by the component of velocity normal to the quarter-chord line in subsonic flight and normal to the leading edge in supersonic flight.

With reference to Fig. 3.19, consider a chordwise section c_h on the right wing panel which is perpendicular to the quarter-chord line. Subsonic flow conditions are assumed, and the flow direction is parallel to the chord line. In the steady equilibrium flight condition the chordwise component of velocity is given by

$$V_c = V_0 \cos\Lambda_{1/4} \tag{3.37}$$

In the presence of a positive sideslip disturbance this becomes

$$V_c{}' = \frac{V_0}{\cos\beta}\cos(\Lambda_{1/4} - \beta) \cong V_0 \cos(\Lambda_{1/4} - \beta) \tag{3.38}$$

where β is the sideslip angle, which is small by definition. Since $V_c' > V_c$, the lift on the right wing panel is increased in sideslip, which creates a negative rolling moment to restore the aircraft to wings-level flight. On the left wing panel there is a corresponding reduction in chordwise velocity in sideslip, which also creates a negative rolling moment. It is therefore evident that wing sweep gives rise to a positive contribution to the lateral static stability of an aircraft.

The fin also contributes to lateral static stability, but its contribution can be stabilising, destabilising, or neutral depending on the steady trim condition when sideslip is experienced. With

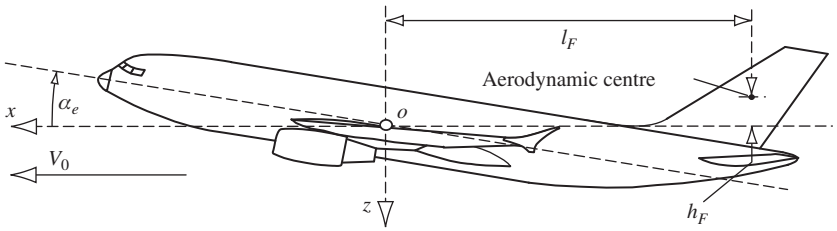

FIGURE 3.20 Fin in sideslip.

reference to Fig. 3.15, when in a sideslip the fin is at incidence to the flow direction equal to the sideslip angle, which causes the fin to generate lift perpendicular to the flow direction. As shown in Fig. 3.20, the fin lift in sideslip acts at the aerodynamic centre of the fin, which may be above or below the roll axis, thereby giving rise to a rolling moment.

With reference to Chapter 13 (Section 13.3.2), it is shown from equation (13.108) that the lateral static stability contribution due to the fin is given by

$$\frac{\mathrm{d}C_l}{\mathrm{d}\beta_{fin}} = -\overline{V}_F \frac{h_F}{l_F} a_{1_F} \tag{3.39}$$

where a_{1_F} is the fin lift curve slope and the *fin volume ratio* is given by

$$\overline{V}_F = \frac{S_F l_F}{Sb} \tag{3.40}$$

When the aerodynamic centre of the fin is above the roll axis, h_F is positive and the expression given by equation (3.39) is negative and hence stabilising. However, it is evident that, depending on aircraft geometry, h_F may be small and may even change sign at extreme aircraft attitude. Thus the fin contribution to lateral static stability varies with trimmed aircraft attitude and may become positive and hence destabilising at low-speed flight conditions.

A number of additional aerodynamic properties of an aircraft can be identified which contribute to lateral static stability in both stabilising and destabilising senses. However, these contributions are often difficult to quantify in terms of simple aerodynamic properties and can only be evaluated by experiment or by complex analysis. For example, a significant contribution arises from the geometry since, in a sideslip disturbance, the lateral cross-flow in the vicinity of the wing root gives rise to differential wing lift, which in turn gives rise to rolling moment. In particular, a high-wing configuration makes a stabilising contribution to lateral static stability whereas a low-wing configuration makes a destabilising contribution. This explains why many high-wing aircraft have little or no dihedral while low-wing configurations often have significant dihedral. Once again, this is an example of how dihedral is used to "tune" the overall lateral static stability of an aircraft. This topic is discussed in a little more detail in Chapter 13 (Section 13.3.2).

As can be seen, the lateral static stability of an aircraft is the sum total of all the contributions. It is extremely important in determining the roll control characteristics of the aircraft and is probably one of the most difficult derivative characteristics to estimate reliably by means of simple analysis alone.

3.4.2 Directional static stability

Directional static stability is concerned with the ability of the aircraft to yaw or *weathercock* into wind in order to maintain directional equilibrium. Since all aircraft are required to fly with zero sideslip in the yaw sense, positive directional stability is designed in from the outset. The fin is the most visible contributor to directional static stability, although, as in the case of lateral stability, there are many other contributions, some of which are destabilising. Again, it is useful to remember that too much directional static stability results in an aircraft that is reluctant to manoeuvre directionally, so obtaining the correct degree of stability is important.

Consider an aircraft that is subject to a positive sideslip disturbance as shown in Fig. 3.21. The combination of sideslip velocity v and axial velocity component U results in a positive sideslip angle β. Note that a positive sideslip angle equates to a negative yaw angle since the nose of the aircraft has swung to the left of the resultant total velocity vector V. In the disturbance, as shown in Fig. 3.21, the fin is at a nonzero angle of attack equivalent to the sideslip angle β. It therefore generates lift L_F, which acts in the sense shown, thereby creating a positive yawing moment N. The yawing moment is stabilising since it causes the aircraft to yaw to the right until the sideslip angle

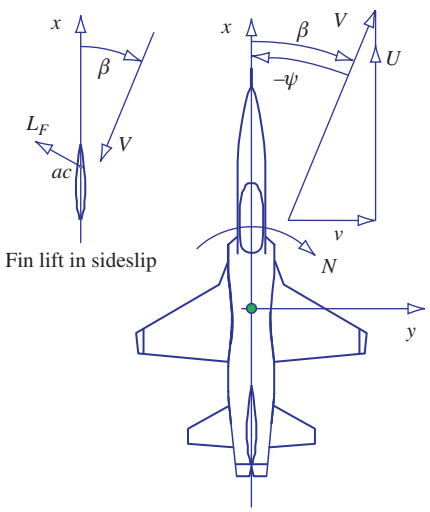

FIGURE 3.21 Directional weathercock effect.

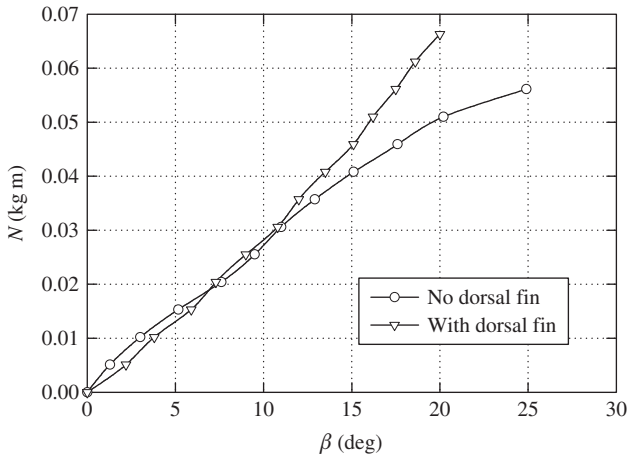

FIGURE 3.22 Plot of yawing moment against sideslip for a stable aircraft.

is reduced to zero. The condition for an aircraft to be directionally stable is thus readily established:

$$\frac{dC_n}{d\beta} > 0 \text{ or, equivalently, } \frac{dC_n}{d\psi} < 0 \tag{3.41}$$

where C_n is the yawing moment coefficient.

A typical plot of yawing moment against sideslip angle for a directionally stable aircraft is given in Fig. 3.22. It shows the results of a wind tunnel test on a simple conventional aircraft model. For small disturbances in yaw the plot is reasonably linear since it is dominated by the lifting properties of the fin. However, as the fin approaches the stall its lifting properties deteriorate and other influences begin to dominate, resulting ultimately in loss of directional stability. The main destabilising contribution comes from the fuselage, which at small yaw angles is masked by the powerful fin effect. The addition of a dorsal fin significantly delays the onset of fin stall, thereby enabling directional static stability to be maintained to higher yaw disturbance angles as indicated in Fig. 3.22.

Fin effectiveness also deteriorates with increasing body incidence angle since the base of the fin becomes increasingly immersed in the fuselage wake, which reduces its effectiveness. This problem has become particularly evident in a number of modern combat aircraft. Such aircraft typically have two engines mounted side by side in the rear fuselage. This results in a broad flat fuselage ahead of the fin, creating a substantial wake which dramatically reduces fin effectiveness at moderate to high angles of incidence. For this reason, many aircraft of this type have noticeably large fins and in some cases have two fins attached to the outer edges of the upper rear fuselage.

Additional sources of yawing moment in sideslip that contribute to the overall directional static stability of the aircraft may be identified, although they may not be so easy to quantify. For

example, as shown in Fig. 3.16 and Fig. 3.19, dihedral effect gives rise to differential lift across the wing span when in a sideslip disturbance. The associated differential-induced drag generates a yawing moment which usually gives rise to a contribution to directional static stability. The side area of the fuselage, especially in very large aircraft, also makes some contribution to directional static stability. The side area ahead of and aft of the *cg* generates yawing moment in sideslip, and the magnitude and sign depend on the distribution of side area about the *cg*. Typically, the yawing moment due to sideslip arising from the side area is often negative and hence destabilising. These contributions to directional static stability are also discussed in more detail in Chapter 13 (Section 13.3.2).

Once again, the directional static stability of an aircraft is the sum total of all contributions. It is extremely important in determining the ability of the aircraft to fly straight and to manoeuvre in yaw, and it is also difficult to estimate reliably by means of simple analysis.

3.5 Calculation of aircraft trim condition

As described in Section 3.1, the condition for an aircraft to remain in steady trimmed flight requires that the forces and moments acting on it sum to zero and that it is stable. Thus in calculating the trim condition of an aircraft it is convenient to assume straight, or symmetric, flight and to apply the principles described earlier in this chapter. For a given aircraft mass, *cg* position, altitude, and airspeed, symmetric trim is described by the aerodynamic operating condition—namely, angle of attack, thrust, pitch attitude, elevator angle, and flight path angle. Other operating condition parameters can then be derived as required.

The forces and moments acting on an aeroplane in the general case of steady symmetric climbing flight are shown in Fig. 3.23, where the symbols have their usual meanings. Since the aircraft is symmetric, the lateral-directional forces and moments are assumed to remain in equilibrium throughout, so the problem reduces to the establishment of longitudinal equilibrium only. Thus, the reference axes are aircraft body axes which define the plane of symmetry *oxz*, with the origin *o* located at the aircraft *cg* as shown.

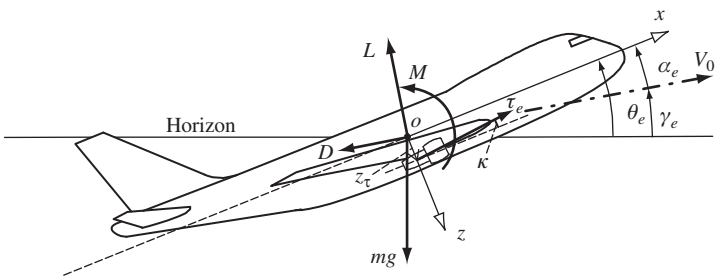

FIGURE 3.23 Symmetric forces and moments acting on a trimmed aircraft.

3.5.1 Defining the trim condition

The total axial force X is given by resolving the total lift L, total drag D, weight mg, and thrust τ_e into the ox axis; these components must sum to zero in trim. Whence

$$X = L\sin\alpha_e + \tau_e\cos\kappa - D\cos\alpha_e - mg\sin(\alpha_e + \gamma_e) = 0 \tag{3.42}$$

where α_e is the equilibrium body incidence, γ_e is the steady flight path angle, and κ is the inclination of the thrust line to the ox body axis (positive nose up). Similarly, the total normal force Z is given by resolving the forces into the oz axis which must also sum to zero in trim. Whence

$$Z = mg\cos(\alpha_e + \gamma_e) - L\cos\alpha_e - D\sin\alpha_e - \tau_e\sin\kappa = 0 \tag{3.43}$$

The development of the aerodynamic pitching moment about the cg is described in Section 3.2 and is given by equation (3.6). However, since the total pitching moment is required, equation (3.6) must be modified to include the thrust and any other significant moment contributions. As before, the total drag moment is assumed insignificant since the normal displacement between the cg and aerodynamic centre is typically small for most aircraft configurations. Also, the tailplane zero-lift pitching moment M_T is assumed small since the aerofoil section is usually symmetrical; and the tailplane drag moment is also very small since the tailplane setting would be designed to trim at a small local incidence angle. Thus the total pitching moment about the cg is given by the sum of the wing-body, tailplane, and thrust moments, which must sum to zero in trim. Whence

$$M = M_0 + L_w(h - h_0)\bar{\bar{c}} - L_T l_T + \tau_e z_\tau = 0 \tag{3.44}$$

where L_w is the wing-body lift and L_T is the tailplane lift. The other symbols are evident from Fig. 3.23.

It is convenient to write equations (3.42) through (3.44) in coefficient form:

$$\frac{mg}{\frac{1}{2}\rho V_0^2 S}\sin(\alpha_e + \gamma_e) = C_\tau\cos\kappa + C_L\sin\alpha_e - C_D\cos\alpha_e \tag{3.45}$$

$$\frac{mg}{\frac{1}{2}\rho V_0^2 S}\cos(\alpha_e + \gamma_e) = C_L\cos\alpha_e + C_D\sin\alpha_e + C_\tau\sin\kappa \tag{3.46}$$

$$C_m = C_{m_0} + (h - h_0)C_{L_w} - \overline{V}_T C_{L_T} + \frac{z_\tau}{\bar{\bar{c}}}C_\tau = 0 \tag{3.47}$$

where the thrust coefficient is given by

$$C_\tau = \frac{\tau_e}{\frac{1}{2}\rho V_0^2 S} \tag{3.48}$$

the total lift coefficient is given by

$$C_L = C_{L_w} + \frac{S_T}{S}C_{L_T} \tag{3.49}$$

and the total drag coefficient is given by

$$C_D = C_{D_0} + \frac{1}{\pi A e}C_L^2 \equiv C_{D_0} + KC_L^2 \tag{3.50}$$

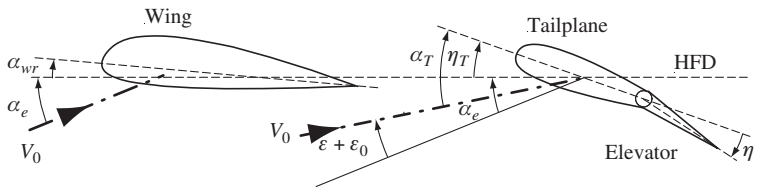

FIGURE 3.24 Practical wing-tailplane aerodynamic geometry.

The wing-body lift coefficient, which is assumed to comprise wing aerodynamic properties only, is given by

$$C_{L_w} = a(\alpha_w - \alpha_{w_0}) \equiv a(\alpha_e + \alpha_{wr} - \alpha_{w_0}) \tag{3.51}$$

where α_{wr} is the wing rigging angle as shown in Fig. 3.24 and α_{w_0} is the zero-lift angle of attack of the wing.

Simultaneous solution of equations (3.45) through (3.51) for a given flight condition determines the values of the aerodynamic coefficients and the body incidence defining the aircraft trim state.

3.5.2 Elevator angle to trim

Once the trim condition is determined, the important elevator angle to trim can be derived along with other useful trim variables. However, the basic aerodynamic relationships described earlier represent the simplest possible definitions in the interests of functional visibility. For a practical aircraft application, it is necessary to take additional contributions into account when assembling the defining equations. For example, the wing-tail aerodynamic relationship is modified by the constraints of a practical layout as illustrated in Fig. 3.24, which is of course a modified version of Fig. 3.9 that includes the wing rigging angle α_{wr} and a zero-lift downwash term ε_0.

The aircraft-fixed reference for the angle definitions is the *horizontal fuselage datum* (HFD), which is usually a convenient *base line*, or *centre line*, for the aircraft geometric layout. It is convenient to define the aircraft *ox* body axis parallel to the HFD, with its origin located at the *cg*; this is shown in Fig. 3.25.

With reference to Fig. 3.24, wing angle of attack is given by

$$\alpha_w = \alpha_e + \alpha_{wr} \tag{3.52}$$

and tailplane angle of attack is given by

$$\alpha_T = \eta_T + \alpha_e - \varepsilon - \varepsilon_0 = \eta_T + \alpha_w - \alpha_{wr} - \varepsilon - \varepsilon_0 \tag{3.53}$$

With reference to equation (3.10),

$$\alpha_w - \varepsilon = \alpha_w \left(1 - \frac{\mathrm{d}\varepsilon}{\mathrm{d}\alpha}\right) \tag{3.54}$$

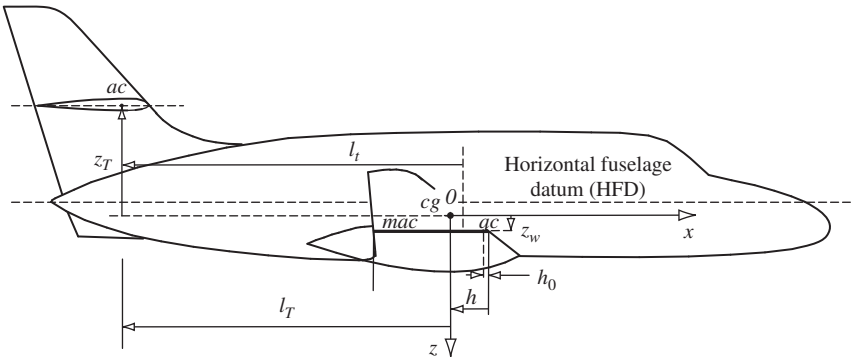

FIGURE 3.25 Practical aircraft longitudinal geometry.

and equation (3.53) may be written as

$$\alpha_T = \eta_T + \alpha_w\left(1 - \frac{\mathrm{d}\varepsilon}{\mathrm{d}\alpha}\right) - \alpha_{wr} - \varepsilon_0 \tag{3.55}$$

It is assumed that the elevator trim tab angle is zero and that aircraft trim is determined by the elevator angle to trim η_e. As before, it is assumed that $a_0 = 0$ since the tailplane aerofoil section is typically symmetrical. The tailplane lift coefficient given by equation (3.8) may therefore be restated with the appropriate substitution of equation (3.55):

$$C_{L_T} = a_1\alpha_T + a_2\eta_e = a_1\left(\eta_T + \alpha_w\left(1 - \frac{\mathrm{d}\varepsilon}{\mathrm{d}\alpha}\right) - \alpha_{wr} - \varepsilon_0\right) + a_2\eta_e \tag{3.56}$$

The elevator angle to trim thus follows by rearrangement of equation (3.56):

$$\eta_e = \frac{C_{L_T}}{a_2} - \frac{a_1}{a_2}\left(\eta_T + \alpha_w\left(1 - \frac{\mathrm{d}\varepsilon}{\mathrm{d}\alpha}\right) - \alpha_{wr} - \varepsilon_0\right) \tag{3.57}$$

Note that equation (3.57) is equivalent to equation (3.13).

3.5.3 Controls-fixed static stability

The location of the controls-fixed neutral point on the mean aerodynamic chord and the controls-fixed static margin are very important parameters in any aircraft trim assessment, since they both influence the aerodynamic, thrust, and control requirements for achieving trim. In practice, the achievement of a satisfactory range of elevator angles to trim over the flight envelope is determined by the static margin, and this in turn places constraints on the permitted range of *cg* positions. The neutral point usually determines the most aft *cg* limit in a stable aircraft. Fortunately, the simple

expressions given by equations (3.17) and (3.18) are sufficient for most practical assessment, and they are repeated here for convenience. The neutral point location h_n is given by

$$h_n = h_0 + \overline{V}_T \frac{a_1}{a}\left(1 - \frac{d\varepsilon}{d\alpha}\right) \tag{3.58}$$

and the static margin K_n is given by

$$K_n = h_n - h \tag{3.59}$$

Estimation of the wing-body aerodynamic centre location h_0 on the mean aerodynamic chord requires careful consideration. For a subsonic wing, typically $h_0 = 0.25$. For the purpose of illustrating the simple theory in Section 3.3, this value is often assumed, incorrectly, to apply to a wing-body combination. However, the presence of the fuselage usually causes a forward shift of the combined wing-body aerodynamic centre to a value more like $h_0 = 0.1$ or less. Clearly, this has an impact on the requirements for trim, and it is important to obtain the best estimate of its location. This can be done by wind tunnel tests on a wing-body combination or, more conveniently, by reference to empirical data sources. Estimation of h_0 is described in ESDU 92024, Volume 4b (ESDU, 2006).

Estimation of the rate of change of downwash angle at the tail with wing angle of attack is another parameter that requires careful estimation, and for the same reasons. Typical values are in the region of $d\varepsilon/d\alpha \approx 0.5$, but the geometric location of the tailplane with respect to the wing strongly influences the actual value. Again, a value can be estimated by wind tunnel testing of a suitable model. Alternatively, $d\varepsilon/d\alpha$ can be estimated with the aid of ESDU 80020, Volume 9a (ESDU, 2006). A simple computer program for estimating $d\varepsilon/d\alpha$ may be found in Stribling (1984), and the use of this program is illustrated in the next section.

3.5.4 "AeroTrim": A Mathcad trim program

A computer program called "AeroTrim" has been written by the author in the Mathcad language to implement the trim calculations described previously; a listing is given in Appendix 1. Since Mathcad permits the development of programs in the format of a mathematical document, the listing is easy to read and is self-explanatory. Because of its computational visibility, Mathcad is an ideal tool for programs of this type, although the program could be written in a number of alternative languages.

AeroTrim is a simple generic trim calculator limited to subsonic flight at altitudes up to 36,000 ft. However, it is very easy for the user to modify the program to suit particular requirements, and it should be regarded as a foundation for such further development. Indeed, the author has produced versions of the program to deal with transonic flight conditions and aircraft performance, and versions can be substantially extended to include aerodynamic derivative estimation.

As listed in Appendix 1, AeroTrim includes numerical data for the Cranfield University National Flying Laboratory Centre (NFLC) Jetstream 31 aircraft. To use it for other aircraft applications it is necessary only to delete and replace the numerical data where prompted to do so. Although based on simple mathematical models, the program produces plausible estimates for the known trim characteristics of the Jetstream, but the small differences from observed practice are thought to be due mainly to propeller effects, which are notoriously difficult to model adequately.

With the program loaded into Mathcad, operation is as simple as clicking on the Calculate button. The impact on trim of changing one or more of the numerical input values can thus be evaluated instantaneously. Points to note include the following:

Section 1. The user inputs flight condition data for which a trim evaluation is required.
Section 2. The program calculates atmospheric temperature, air density, and density ratio for the chosen altitude based on the ISA model. It is currently limited to the troposphere, but is easily modified to include the stratosphere.
Section 3. The user defines the velocity range over which the trim conditions are required, bearing in mind that the computations are valid only for subsonic flight conditions. The counter sets the number of velocity steps through the range, currently set at 10. The range expression sets the starting velocity, currently set at 100 knots, and the increment, currently set at 15 knots.
Section 4. The user inserts values for the aircraft geometry constants, taking care to observe the body axis system used. All of this information would be readily available in a three-dimensional drawing of the aircraft.
Section 5. The user inputs values for the principal wing-body aerodynamic parameters for the aircraft. Unknowns obviously have to be estimated by whatever means are available.
Section 6. The user inputs values for the tailplane aerodynamic parameters. Again, unknowns have to be estimated by whatever means are available.
Section 7. The program calculates some basic wing-body-tail parameters.
Section 8. The program estimates $d\varepsilon/d\alpha$ for the given aircraft geometry using a simple algorithm described by Stribling (1984). Since the model does not include fuselage interference effects or thrust effects, it may underestimate the parameter by a small amount. However, results obtained with the algorithm seem to be plausible and appropriate.
Section 9. The program estimates the induced-drag factor K in the drag polar $C_D = C_{D_0} + KC_L^2$ using an empirical method described in Shevell (1983), which is based on industrial flight test experience. The very limited data for the fuselage drag factor s_d and the empirical constant k_D were plotted and curves were fitted to give expressions suitable for inclusion in the computation. Results obtained for the Jetstream compare very favourably with the known drag properties of the aircraft.
Section 10. The program calculates some useful standard performance and stability parameters.
Section 11. The program calculates the trim conditions, solving equations (3.45) through (3.51) simultaneously for each velocity step defined in Section 3.
Section 12. The program calculates the dependent trim variables, including elevator angle, for the velocity steps defined in Section 3 and using the results of Section 11.
Sections 13 and 14. These are self-explanatory auxiliary computations.
Section 15. Results: The program gives a summary of the flight condition parameters for the chosen application.
Section 16. Results: The program gives a tabulated summary of the trim values of all variables at each velocity step in the range chosen.
Section 17. Results: the program shows some plotted variables to illustrate the kind of output Mathcad can provide. It is very easy to edit this section to include plots of any variables from the table in Section 16.

EXAMPLE 3.4

To illustrate the use of AeroTrim the program is applied to the NFLC Jetstream 31 aircraft. Since a comprehensive flight simulation model of the aircraft has been assembled and matched to observed flight behaviour, the numerical data are believed to be reasonably representative. The sources of data used include manufacturers' published technical information, the flight manual, limited original wind tunnel test data, and data obtained from flight experiments. Aerodynamic data not provided by any of these sources were estimated using the ESDU Aerodynamics Series (ESDU, 2006) and refined by reference to observed flight behaviour. The numerical data are not listed here since they are illustrated in the Mathcad listing in Appendix 1.

The chosen operating condition is typical for the aircraft, and the speed range was chosen to vary from the stall, at around 100 knots, to 250 knots in 15-knot increments. Good-quality data for the remaining input parameters were available, with the possible exception of the values for wing-body aerodynamic centre position h_0 and the rate of change of downwash at the tail with wing angle of attack $d\varepsilon/d\alpha$. Both parameters were estimated for the aircraft, although the actual

Flight Condition	Units	Value
Aircraft weight	kN	61.8
Altitude	ft	6562
Flight path angle	deg	0
cg position		0.29
Neutral point		0.412
Static margin		0.122
Minimum drag speed	knots	150
Stall speed	knots	116

Example Trim Data

V_{true} (knots)	C_L	C_D	C_τ	L/D	α_e (deg)	η_e (deg)	L (kN)	D (kN)	τ_e (kN)
100	1.799	0.174	0.181	9.409	15.105	-1.208	60.23	5.834	6.042
115	1.374	0.114	0.116	11.017	10.885	-0.460	60.83	5.053	5.146
130	1.081	0.082	0.083	12.106	7.970	0.100	61.15	4.643	4.688
145	0.872	0.064	0.064	12.603	5.885	0.521	61.34	4.494	4.518
160	0.717	0.053	0.053	12.573	4.346	0.842	61.46	4.535	4.548
175	0.600	0.046	0.046	12.154	3.181	1.091	61.54	4.722	4.729
190	0.510	0.042	0.042	11.496	2.277	1.287	61.60	5.025	5.029
205	0.438	0.039	0.039	10.720	1.564	1.444	61.65	5.424	5.426
220	0.381	0.036	0.036	9.912	0.990	1.572	61.70	5.907	5.908
235	0.334	0.035	0.035	9.123	0.523	1.677	61.74	6.465	6.465
250	0.295	0.034	0.034	8.383	0.136	1.764	61.79	7.089	7.089

value for $d\varepsilon/d\alpha$ is thought to be larger than that estimated by the program. Using the value $d\varepsilon/d\alpha = 0.279$ as calculated, the value of $h_0 = -0.08$ was estimated since it returned values for the neutral point position h_n and static margin K_n close to their known values. It is likely that this places the aerodynamic centre too far forward in the aircraft. However, with a value of $d\varepsilon/d\alpha$ nearer to its probable value, $d\varepsilon/d\alpha \cong 0.4$, a more aft aerodynamic centre position would return the known stability properties. This illustrates one of the difficulties of gathering reliable aerodynamic data for an aircraft. For unconventional configurations the difficulties are generally greater. Running the program returns trim data for the chosen operating flight condition, of which a reduced selection is shown.

For the purpose of trim analysis, the data can be graphed as required, and some examples are given in the Mathcad program listing. It follows that the effect of any aerodynamic variable on aircraft design performance can be evaluated quickly using the program. Indeed, this approach was used to identify plausible values for some of the more uncertain values in the model definition.

References

Babister, A. W. (1961). *Aircraft stability and control.* London: Pergamon Press.

Cook, M. V. (1994). The theory of the longitudinal static stability of the hang-glider. *Aeronautical Journal*, *98*, 978.

Duncan, W. J. (1959). *The principles of the control and stability of aircraft.* Cambridge, UK: Cambridge University Press.

ESDU (2006). *ESDU aerodynamics series.* London: IHS ESDU International, www.esdu.com.

Gates, S. B., & Lyon, H. M. (1944). *A continuation of longitudinal stability and control analysis: Part 1, general theory*, Reports and Memoranda No. 2027, Aeronautical Research Council. Her Majesty's Stationery Office, London.

Shevell, R. S. (1989). *Fundamentals of flight* (2nd ed.). Englewood Cliffs, NJ: Prentice Hall, USA.

Storey, R. F. R. (1966). *H.P.137. Longitudinal and lateral stability measurements on a 1/6th scale model,* W.T. Report No. 3021. Weybridge: Surrey: BAC (Operating) Ltd.

Stribling, C. B. (1984). *Basic aerodynamics.* London: Butterworth & Co.

Source

Mathcad. Adept Scientific, Amor Way, Letchworth, Herts, SG6 1ZA. <www.adeptscience.co.uk>.

PROBLEMS

3.1 Explain why the pitching moment coefficient $C_{m_{ac}}$ about the aerodynamic centre of an aerofoil is constant. What is the special condition for $C_{m_{ac}}$ to be zero?

The NACA 64-412 is a cambered aerofoil with lift coefficient given by

$$C_L = 0.11\alpha + 0.3$$

where α is in degree units. What is the value of the constant pitching moment coefficient about the aerodynamic centre? Estimate the position of the centre of pressure for the aerofoil at an angle of attack of 5 deg. State all assumptions made in answering this question.

(CU 1998)

3.2 What are the conditions for the stable longitudinal trim equilibrium of an aircraft? The pitching moment coefficient about the *cg* for a stable aircraft is given by

$$C_m = C_{m_0} + C_{L_w}(h - h_0) - \overline{V}_T\left(C_{L_w}\frac{a_1}{a}\left(1 - \frac{\mathrm{d}\varepsilon}{\mathrm{d}\alpha}\right) + a_2\eta\right)$$

where the symbols have the usual meaning. Derive expressions for the controls-fixed static margin K_n and the elevator angle to trim as a function of static margin. Explain the physical meaning of the controls-fixed neutral point.

(CU 1998)

3.3 State the conditions required for an aircraft to remain in longitudinal trimmed equilibrium in steady level flight. The pitching moment equation, referred to the centre of gravity (*cg*), for a canard-configured combat aircraft is given by

$$C_m = C_{m_0} + (h - h_0)C_{L_{wb}} + \overline{V}_f\left(\frac{a_{1_f}}{a_{wb}}C_{L_{wb}} + a_{1_f}\delta\right)$$

where the symbols have the usual meaning; additionally, $\overline{V}_f$ is the foreplane volume ratio, a_{1_f} is the foreplane lift curve slope, and δ is the control angle of the all-moving foreplane.

(a) Derive expressions for the controls-fixed static margin and for the controls-fixed neutral point. State any assumptions made.

(b) Given that the mean aerodynamic chord (*mac*) is 4.7 m, the wing-body aerodynamic centre is located at 15% of *mac*, the foreplane volume ratio is 0.12, and the lift curve slopes of the wing-body and foreplane are 3.5 rad^{-1} and 4.9 rad^{-1}, respectively, calculate the aft *cg* limit for the aircraft to remain stable with controls fixed. Calculate also the *cg* location for the aircraft to have a controls-fixed static margin of 15%.

(CU 1999)

3.4 Sketch a typical $C_m - \alpha$ plot and explain the condition for trim, the requirement for static stability, and the concept of stability margin. Why is too much stability as hazardous as too little? (CU 2001)